

**Enumeration of Novel Lake Superior Cluster I  
(LSI) as a Fraction of the Total Picocyanobacteria in  
the Autotrophic Picoplankton (APP) using  
Quantitative Real-Time PCR**

by

Jihad C. El Andari

**A thesis submitted in partial fulfillment  
of the requirements for the degree of**

Master of Science

Molecular Biology

Lebanese American University

2009-10

**Under the supervision of**

**Dr. Brigitte Wex**

I grant to the **LEBANESE AMERICAN UNIVERSITY** the right to use this work, irrespective of any copyright, for the University's own purpose without cost to the University or to its students, agents and employees. I further agree that the University may reproduce and provide single copies of the work, in any format other than in or from microfilms, to the public for the cost of reproduction.

Jihad C. El Andari

## **Plagiarism Policy Compliance Statement**

I certify that I have read and understood LAU's Plagiarism Policy. I understand that failure to comply with this Policy can lead to academic and disciplinary actions against me. This work is substantially my own, and to the extent that any part of this work is not my own I have indicated that by acknowledging its sources.

Jihad C. El Andari

# LEBANESE AMERICAN UNIVERISTY

## ABSTRACT

### **Enumeration of Novel Lake Superior Cluster I (LSI) as a Fraction of the Total Picocyanobacteria in the Autotrophic Picoplankton (APP) using Quantitative Real-Time PCR**

by Jihad C. El Andari

Cyanobacteria known previously as blue-green algae are successful phototrophic organisms which are ubiquitously found in the environment. This organism contributes significantly to the global carbon and nitrogen budget. Classical classification of cyanobacteria is mainly based on morphology and subdivided into five categories. Molecular classification involves mainly 16S rRNA, 16S-23S rRNA intergenic spacer (IGS), and *cpcBA* IGS. Planktonic organisms are separated in literature based on size. We are primarily interested in picocyanobacteria (picos) as major fraction of the autotrophic picoplankton (APP) that are ubiquitously found in all aquatic ecosystems. They are major contributors of carbon and provide nutrients to their natural habitats through complex microbial food webs. Lake Superior is located in North America and has the largest surface area of any freshwater lake present in the world. The nature of this lake is ultraoligotrophic with very low concentrations of iron and phosphorous. Although 50% of Lake Superior chlorophyll is contributed by the APP, only few studies focused on studying the biodiversity of this lake. The phylogenetic diversity of Lake Superior picos was recently characterized. All samples were collected and filtered from several locations and at different depths including Sterner B (SB), Castle Danger 1 (CD1), Western Mid-lake (WM), and nearshore Keweenaw Waterway station Portage Deep

(PD). Most of the 16S rRNA gene sequences clustered within the picocyanobacterial clade and two new groups pelagic Lake Superior clusters I (LSI) and II (LSII) were discovered. These groups do not cluster with any of the previously known freshwater *Synechococcus*. Also, these novel groups have never been isolated into culture. In our study, we assessed LSI and general picos by quantitative real-time PCR (qPCR). Specific PCR amplicons of LSI and picos were cloned into plasmid and transformed into *E. coli* competent cells for multiplication of the plasmid. Two separate standard curves were created for specific quantification. The concentration of general picos at CD1 (September, 2004) was found to be in the range of flow cytometry results shown by Ivanikova *et al.* (2007) of phycocyanin-rich and phycoerythrin-rich APP collected from the same location (August, 2006). Although Ivanikova *et al.* (2007) found that 16S rRNA sequences that clusters within LSI were less abundant at PD, similar and even higher concentrations of LSI were detected at this station compared to CD1, WM, and SB. WM samples collected from deep chlorophyll maximum (DCM) showed approximately the same concentrations of LSI as CD1 and PD samples collected from the epilimnion. Generally, LSI at PD and WM showed higher levels whereas picos were more concentrated at CD1 and WM. LSI proportions of picos at CD1, WM, and SB were 4.4 %, 24%, and 15.5% respectively. This study provides valuable information about the dynamics of the picos at the western arm of Lake Superior. Moreover, specific and sensitive qPCR protocol created in this study can be used in future work to monitor the spatial and temporal abundance of picos and LSI.

<b>TABLE OF CONTENTS</b>	<b>Page</b>
List of Figures .....	iv
List of Tables .....	vi
Glossary.....	vii
Acknowledgments .....	viii
<b>1. INTRODUCTION .....</b>	<b>1</b>
<b>1.1 Cyanobacteria.....</b>	<b>1</b>
<b>1.2 Classical classification of cyanobacteria .....</b>	<b>3</b>
<b>1.3 Molecular classification of cyanobacteria .....</b>	<b>3</b>
<b>1.4 Mechanisms of adaptation in cyanobacteria .....</b>	<b>4</b>
<b>1.5 Planktonic organisms separated based on size.....</b>	<b>7</b>
<b>1.6 Autotrophic picoplankton (APP).....</b>	<b>9</b>
<b>1.7 Single-cell picocyanobacteria.....</b>	<b>10</b>
<b>1.8 Colonial picocyanobacteria.....</b>	<b>13</b>
<b>1.9 APP dynamics.....</b>	<b>15</b>
<b>1.10 Advances used in the classification of cyanobacteria.....</b>	<b>17</b>
<b>1.10.1 Epifluorescence and pigmentation.....</b>	<b>17</b>
<b>1.10.2 Quantitative real-time PCR (qPCR).....</b>	<b>19</b>
<b>1.11 Lake Superior as a model of ultraoligotrophic lake.....</b>	<b>20</b>
<b>1.12 <i>Synechococcus</i> sp. and novel Lake Superior cluster I (LSI) and II         (LSII).....</b>	<b>22</b>
<b>1.13 Specific quantitative real-time PCR (qPCR) of Lake Superior         Cluster I (LSI).....</b>	<b>27</b>
<b>2. MATERIALS AND METHODS .....</b>	<b>28</b>
<b>2.1 Sample collection.....</b>	<b>28</b>

2.2	Genomic DNA extraction.....	29
2.3	PCR Amplification.....	29
2.3.1	Primers.....	30
2.3.2	PCR conditions and reagents.....	30
2.4	Cloning Procedures.....	31
2.4.1	PCR.....	31
2.4.2	DNA purification from agarose gel.....	31
2.4.3	Cloning reactions.....	31
2.4.4	Screening for transformants .....	32
2.4.5	Plasmid DNA Extraction.....	32
2.4.6	Amplification of the ligated PCR insert.....	32
2.5	Sequencing.....	32
2.5.1	Pre-sequencing PCR.....	33
2.5.2	Purification (ExoSAP-IT, modified methodology).....	33
2.5.3	Sequencing PCR.....	33
2.5.3.1	DNA precipitation (Dye-Ex).....	34
2.5.3.2	Loading and Processing.....	34
2.5.3.3	Data analysis.....	34
2.6	Quantitative real-time PCR (qPCR).....	35
<b>3.</b>	<b>RESULTS .....</b>	<b>37</b>
3.1	LSI 261R primer sensitivity.....	37
3.2	Cloning and sequencing gels.....	38
3.3	Specificities of general picos and LSI qPCR.....	41
3.4	General picos and LSI gene copy numbers of the 16S rRNA per mL of filtered water from Lake Superior.....	50

<b>4. DISCUSSION .....</b>	<b>52</b>
<b>4.1 qPCR standard curves and melting curve analysis.....</b>	<b>52</b>
<b>4.2 Distribution of general picos and LSI in Lake Superior.....</b>	<b>55</b>
<b>4.3 Conclusion .....</b>	<b>56</b>
<b>4.4 Future outlook.....</b>	<b>56</b>
<b>5. BIBLIOGRAPHY .....</b>	<b>58</b>



## LIST OF FIGURES

Figure	Page
1. Simple plasmids originated by primary endosymbiosis .....	2
2. Schematic overview of the freshwater cyanobacteria <i>Synechococcus elongates</i> nitrate assimilation system .....	6
3. Photomicrograph showing a picocyanobacterium cell undergoing division .....	8
4. Epifluorescence microscopy image with 787.7x magnification showing <i>Vorticella</i> sp.....	10
5. Phylogenetic tree representing the maximum of likelihood the picophytoplankton clade sensu Urbach <i>et al.</i> (1998) .....	14
6. Cultures of <i>Synechococcus</i> sp. ....	18
7. Flow cytometry of water samples collected from CD1 .....	25
8. Phylogenetic tree inferred from the 615 bases of the 16S rRNA sequences from samples collected at CD1 station .....	26
9. Map of the western arm of Lake Superior showing hydrographic locations.....	29
10. Amplification with CYA 107F and LSI 261R primers showed by 1% agarose gel electrophoresis.....	37
11. Pre-sequencing PCR with M13 Forward and M13 Reverse primers of cloning construct .....	38
12. Consensus sequence of both M13 Forward and M13 Reverse primers ....	39

<b>13.</b> Amplification of plasmid DNA (20 ng) to confirm successful cloning procedure of LSI .....	40
<b>14.</b> Amplification of plasmid DNA (50 ng) to confirm successful cloning used for building the standard curve of general picos.....	40
<b>15.</b> Real-time PCR amplification graph of standards.....	42
<b>16.</b> Standard curve for qPCR was determined as log concentration (DNA copy numbers / reaction) in correlation to cycle threshold (Ct).....	43
<b>17.</b> Melting curves of standards.....	44
<b>18.</b> Melting curve analysis of standards.....	45
<b>19.</b> qPCR amplification graph of samples.....	46
<b>20.</b> Melting curve analysis of samples.....	48
<b>21.</b> Melting curve analysis of standards used to build the standard curve of general picos with CYA 107F and PICO 224R primers showing slight shift in the melting peaks .....	49
<b>22.</b> Amplification with CYA 107F and PICO 224R viewed by 1% agarose gel electrophoresis showing exact amplicon size.....	49
<b>23.</b> Distribution and correlation of picos and LSI in relation to the same location of Lake Superior .....	51

## LIST OF TABLES

<b>Table</b>	<b>Page</b>
1. Planktonic organisms are described in literature based on their size.....	8
2. Quantification of general picos 16S rRNA gene copy numbers and Ct values were obtained .....	47
3. Quantification of LSI 16S rRNA gene copy numbers and Ct values were obtained .....	47
4. Gene copy numbers (16S rRNA) of general picos and LSI per mL of filtered water .....	50
5. One nucleotide difference in LSI 261R annealing sequence detected from Lake Superior isolates .....	53
6. Sequence variation detected in PICO 224R annealing sequence.....	54

## GLOSSARY

AO: acridine orange  
APP: autotrophic picoplankton  
ATP: adenosine triphosphate  
CD1: Castle Danger 1  
chl-*a*<sub>2</sub>: chlorophyll *a*  
chl-*b*<sub>2</sub>: chlorophyll *b*  
Ct: cycle threshold  
DGGE: denaturing gradient gel electrophoresis  
ds: double stranded  
DCM: deep chlorophyll maximum  
FITC: fluorescein isothiocyanate  
HNF: heterotrophic nanoflagellates  
IGS: intergenic spacer  
LSI: Lake Superior cluster I  
LSII: Lake Superior cluster II  
LB: Luria-Bertani  
N<sub>2</sub>: nitrogen  
NJ: neighbor-joining  
PC: phycocyanin  
PD: Portage Deep  
PE: phycoerythrin  
picos: picocyanobacteria  
qPCR: quantitative real-time PCR  
SB: Sterner B  
SG: SYBR green I  
WM: Western Mid-lake

## ACKNOWLEDGEMENTS

This thesis would not have been accomplished without the supervision, assistance and guardianship of my instructors, colleagues, family and friends. Foremost is my Advisor, Dr. Brigitte Wex, without whom this work could have not have reached the stage of submission for defense. I would like to express my deep appreciation for her dedicated and professional advising.

I would like to thank Dr. George Bullerjahn at Bowling Green State University for providing me with samples and sequences of all cyanobacteria samples obtained by the study undertaken at his university. Also, my deep gratitude goes to Dr. Irina Ilikchyan at the University of California, Santa Cruz who has been helpful in primer design and in giving comments, which contributed to the improvement of my thesis.

I am grateful to Dr. Sima Tokajian, a member of my thesis committee, for her continuous support and for making all microbiology laboratory equipments accessible for me. The same gratitude goes to Dr. Roy Khalaf, the other member of my thesis committee, for his motivating attitude towards me during the long hours I have spent at the graduate laboratory.

Miss Maya Farah has been always generous in providing me with technical advice and help in DNA sequencing. Mrs. Helena Bou Farah must be appreciated for making laboratories a pleasant and organized place to work in. I would like to thank also Marc Haber for his comments on melting peaks. Dr. Mirvat El-Sibai has been always a good listener and a motivating person in the course of my research.

The list of graduate students who have always been supportive and encouraging is quite long. However, I wish to mention here Katia Malouf, Sonia Youhanna, Samer Younis, Jalil Daher, and Wael Bahnan with whom I spent many hours in the laboratory this past year.

Dr. Vahid Behmardi has been a caring mentor and Nassib Saliba a true friend at difficult moments. To both I am always grateful.

Last but not least, my parents Chawki and Heyam, as they have been the cause of my physical existence, they have been the primal cause of any success in my academic life through their endless love and continuous support, notwithstanding my dear sister Sara, therefore,

*I dedicate this modest accomplishment to my parents*

*Chawki and Heyam*

## *Chapter I*

### **INTRODUCTION**

#### **1.1 Cyanobacteria**

Cyanobacteria previously known as blue-green algae are one of the most morphologically diverse phototrophic prokaryote. The phylum Cyanobacteria (Cyanophyta) belongs to the domain Bacteria (Giovannoni *et al.*, 1988). The invention of the electron microscope showed that blue-green algae are well-defined microscopic organisms lacking membrane-bounded organelles. Cyanobacteria are surrounded with exopolysaccharide which covers a cell envelope of Gram-negative bacteria (Mariné *et al.*, 2004). Interestingly, the oldest fossils on earth belong to cyanobacteria manifested in microfossils preserved in the old Apex chert of Western Australia dating 3,460 million years (Brasier *et al.*, 2004). In general, no other earth microorganism has had a more significant impact on the transition process of earth's anaerobic atmosphere to aerobic state approximately 2.3 billion years ago (Shi & Falkowski, 2007; Giovannoni *et al.*, 1988). Cyanobacteria are ubiquitously found in the environment including aquatic and terrestrial, and can survive in extreme habitats such as hot springs, deserts and earth poles (Tomitani *et al.*, 2006). Cyanobacteria contribute significantly to the global primary production, i.e. utilization of atmospheric or aquatic carbon dioxide to produce organic compounds. Furthermore, nitrogen (N<sub>2</sub>)-fixing microorganisms (diazotrophs) contribute to the global nitrogen budget by fixing atmospheric nitrogen to more exploitable forms such as ammonia (Church *et al.*, 2008; Shi and Falkowski, 2007). Cyanobacteria have been the key for understanding several

concepts related to the biological and environmental evolution of earth (Tomitani *et al.*, 2006). The plastids of plants and algae were evolved from cyanobacteria supported by the primary and secondary endosymbiotic theory. Simple plastids which are made of two-bounded membrane were evolved by primary endosymbiosis (Bhattacharya and Medlin, 1998). The chloroplast of plants and algae including chlorophyta (green algae), rhodophyta (red algae), glaucocystophyta were evolved by primary endosymbiosis. On the other hand, complex plastids, three- (or more) bounded membranes present in euglenophyta, heterokonta, haptophyta, cryptophyta, dinoflagellate, and apicomplexan, originated by secondary endosymbiosis of existing algae (Figure 1) (Bhattacharya and Medlin, 1998; Sato *et al.*, 2005).

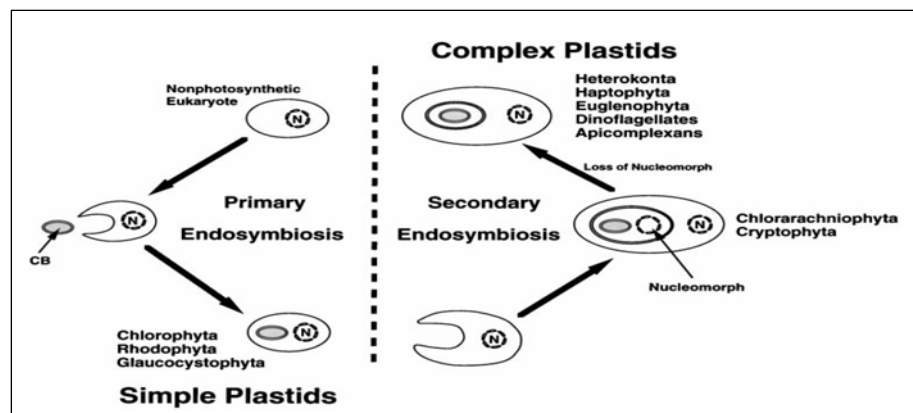


**Figure 1.** Simple plasmids originated by primary endosymbiosis reflecting the two-bounded membrane of cyanobacteria (left). The existing algae was engulfed by another algae supporting the secondary endosymbiosis theory which formed the complex plastids (right), three and more bounding membranes. CB, cyanobacteria; N, nucleus (Bhattacharya and Medlin, 1998). Giovannoni *et al.* (1988) indicates that the chloroplast of algae and higher plants is closely related to cyanobacteria which is consistent with molecular phylogenetic analysis and arrangement of the photosynthetic apparatus in these organisms.



## **1.2 Classical classification of cyanobacteria**

Although cyanobacteria are monophyletic, they were classified morphologically into five subsections. Subsection I (previously Chroococcales) and II (Pleurocapsales) of cyanobacteria are unicellular coccoids. Subsection I reproduce by binary fission, however subsection II undergoes also multiple fission which result in small cells (baeocytes) that are easily dispersed in the environment. Filaments of various morphological complexities are found in subsection III (Oscillatoriales), IV (Nostocales), and V (Stigonematales). Subsection III forms only vegetative cells, whereas subsection IV and V vegetative cells can develop into distinct heterocysts which are specialized cells in nitrogen fixing machinery under aerobic conditions, and akinetes, resting cells that survive harsh environmental conditions such as aridity and cold. Subsection V forms complicated branching filaments (Tomitani *et al.*, 2006).

## **1.3 Molecular classification of cyanobacteria**

Sequence analysis of the 16S rRNA is considered one of the most promising approaches for the molecular classification of cyanobacteria at all taxonomic levels. The gene sequences are not affected by culture conditions and can be amplified from a small amount of extracted DNA of culture or environmental samples (Nubel *et al.*, 1997; Ivanikova *et al.*, 2007). Classifying subsections of cyanobacteria including baeocyte (subsection II), heterocyst (subsections IV and V), and true-branching filament (subsection V) producers based on the 16S rRNA sequences suggest that each subsection is phylogenetically coherent. Conversely, phylogenetic analysis based on nitrogenase structural genes (*nifH* and *nifD*), nitrogenase is the enzyme that catalyzes nitrogen

fixation in some cyanobacteria species, does not support the monophyly of subsection V. Also, phylogeny of *nifH* suggests paraphyly of subsection II. It is noteworthy that not all cyanobacteria have the ability to fix nitrogen; therefore *nifH* and *nifD* are not the best molecular markers for phylogenetic classification. Combination of three genes (16S rRNA, *rbcL*, and *hetR*) was used to investigate the evolution of cell differentiation which reflects the evolution of life on earth. The *rbcL* gene codes for the large subunit of ribulose 1,5-bisphosphate carboxylase/ oxygenase which is the key enzyme for CO<sub>2</sub> fixation in the Calvin cycle, and *hetR* is an essential gene for heterocyst differentiation (Tomitani *et al.*, 2006). Also, *rbcLX* intergenic spacer (IGS) with no identified functional properties was investigated to estimate the evolution rates of cyanobacteria. *rbcL* gene is more conserved in cyanobacteria compared to the *rbcX*, gene of a possible chaperonin-like function. Therefore, *rbcLX* IGS studied reflects both conserved and less conserved regions (Rudi *et al.*, 1998). The 16S-23S rRNA IGS in the ribosomal operon was examined to determine the phycoerythrin (PE)-rich *Synechococcus* sp. diversity of cyanobacteria (Becker *et al.*, 2002; Ernst *et al.*, 2003). Several studies explored the *cpcBA* IGS, as a part of the phycocyanin operon, to examine the genetic diversity of water samples (Crosbie *et al.*, 2003; Manen *et al.*, 2002; Ivanikova, 2007). Haverkamp *et al.* (2008) showed that *cpcBA* was able to differentiate pigmented picocyanobacteria more specifically than 16S-23S rRNA IGS.

#### **1.4 Mechanisms of adaptation in cyanobacteria**

Throughout the long course of evolution, cyanobacteria have developed various mechanisms of adaptation. It is known that nitrogenase is highly

sensitive to molecular oxygen which made cyanobacteria develop temporal and spatial adaptation mechanisms. In the former adaptation, some filamentous cyanobacteria developed the ability to form heterocysts which are non-dividing cells containing nitrogenase; however, lost the activity of oxygenic photosynthesis. Nitrogenase and photosynthesis were shown to occur in the same cell of non-heterocystous filamentous and unicellular nitrogen-fixing cyanobacteria. These cyanobacteria cells, when grown under consecutive dark and light cycles, showed nitrogenase temporal activity only under dark cycles (Stal and Krumbein, 1987). The ability of cyanobacteria to regulate buoyancy with gas vesicles was developed to maintain effective light capturing mechanisms and resist turbulence of water in the vertical water column (Steinberg and Hartmann, 1988; Walsby *et al.*, 1995). Chromatic adaptation of cyanobacteria was attributed to the regulation of the main cellular phycobilins, phycoerythrin (PE) and phycocyanin (PC), which expanded the range of absorption patterns of the visible light spectrum (Erokhina *et al.*, 2004; Marsac, 1977). Cyanobacteria have developed nutrient uptake mechanisms allowing its survival in oligotrophic ecosystems which have a low nutrient content. Freshwater cyanobacteria containing *Synechococcus* and *Prochlorococcus* species utilize nitrate as the nitrogen source for growth (Scanlan and West, 2002). For instance, the process of nitrogen uptake is mediated in *Synechococcus elongates* by ABC transporter. Both ATP and reduced ferredoxin by photosynthesis in cyanobacteria facilitate the uptake of nitrate and its reduction to nitrite and ammonium (Figure 2) (Flores *et al.*, 2009).

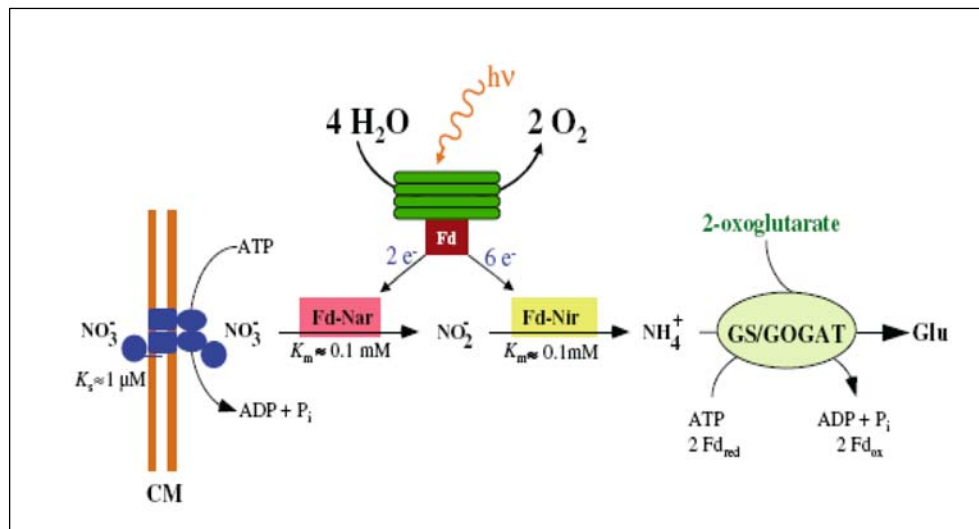


**Figure 2.** Schematic overview of the freshwater cyanobacteria *Synechococcus elongates* nitrate assimilation system. The nitrate/nitrite ABC-type transporter or permease is located at the cytoplasmic membrane (CM). Ferredoxin (Fd) is photosynthetically reduced at the thylakoids and utilized as an electron donor by two enzymes including nitrate reductase (Fd-Nar) and nitrite reductase (Fd-Nir). In the nitrite/nitrate permease, periplasmic substrate-binding protein is anchored to the membrane and two transmembrane subunits and two ATPase subunits are located in the cytoplasmic side of the membrane. As a result of nitrate reduction, ammonium is incorporated into amino acids by the glutamine synthetase/glutamate synthase (GS/GOGAT) pathway in which ATP is consumed and 2-oxoglutarate is used as a final N acceptor (Fd<sub>red</sub>, reduced ferredoxin; Fd<sub>ox</sub>, oxidized ferredoxin).  $K_s$  and  $K_m$  represent the affinity constants of permease and reductases respectively (Flores *et al.*, 2005).

## **1.5 Planktonic organisms separated based on size**

Planktonic organisms can be classified into three major groups consisting of bacterioplankton (referring mainly to heterotrophic prokaryotes), phytoplankton (including cyanobacteria and eukaryotes), and zooplankton (containing eukaryotic unicellular and multicellular organisms). Furthermore, taxonomic, physiological, or dimensional criteria are considered in subdividing planktonic organisms. Some of the prevalent terminology in literature separates organisms based on size including macroplankton (200-2000  $\mu\text{m}$ ), microplankton (20-200  $\mu\text{m}$ ), nanoplankton (2-20  $\mu\text{m}$ ), picoplankton (0.2-2  $\mu\text{m}$ ), and femtoplankton (0.02-0.2  $\mu\text{m}$ ). Further elucidations, as presented in the literature, are described in (Table 1). Prokaryotic organisms (picocyanobacteria) and eukaryotic phototrophs and heterotrophs form the picoplankton (Figure 3) which is ubiquitously distributed world wide in all types of lakes and trophic ecology systems (Callieri and Stockner, 2002). It has been approximately 42 years since the discovery of the picophytoplankton (size range: 0.2  $\mu\text{m}$  to 2  $\mu\text{m}$ ) which consists of the prokaryotic picocyanobacteria and eukaryotic phototrophs. Picophytoplankton terminology is formally used in describing the unicellular members which live solely in the ecosystem; however, microcolonies of 'non-blooming' species, consisting of more than 50 individual cells inhabiting freshwater ecosystems, also belong to picophytoplankton (Callieri, 2007).

**Table 1.** Planktonic organisms are described in literature based on their size (Callieri and Stockner, 2002).

Terminology	Size	References
Net plankton	>45 $\mu\text{m}$ >64 $\mu\text{m}$	Thronsdon 1978 Vollenweider <i>et al.</i> 1974, Ross & Duthie 1981
Microplankton	20 - 200 $\mu\text{m}$ 50 - 500 $\mu\text{m}$ 60 - 500 $\mu\text{m}$	Dussart 1965, Sieburth <i>et al.</i> 1978 Margalef 1955 Hutchinson 1967
Nanoplankton	2 - 20 $\mu\text{m}$ 5 - 50 $\mu\text{m}$ 5 - 60 $\mu\text{m}$ <45 $\mu\text{m}$ <100 $\mu\text{m}$ <64 $\mu\text{m}$ 15 - 64 $\mu\text{m}$	Dussart 1965, Sieburth <i>et al.</i> 1978 Margalef 1955 Hutchinson 1967 Thronsdon 1978 Rodhe 1958 Vollenweider <i>et al.</i> 1974 Ross & Duthie 1981
Ultrananoplankton	<2 $\mu\text{m}$	Dussart 1966
Ultraplankton	<5 $\mu\text{m}$ 0.5 - 5 $\mu\text{m}$ 1 - 10 $\mu\text{m}$ 1 - 15 $\mu\text{m}$ <15 $\mu\text{m}$	Margalef 1955 Hutchinson 1967 Thronsdon 1978 Reynolds 1973 Ross & Duthie 1981
Picoplankton	0.2 - 2 $\mu\text{m}$	Sieburth <i>et al.</i> 1978
Femtoplankton	0.02 - 0.2	Sieburth <i>et al.</i> 1978

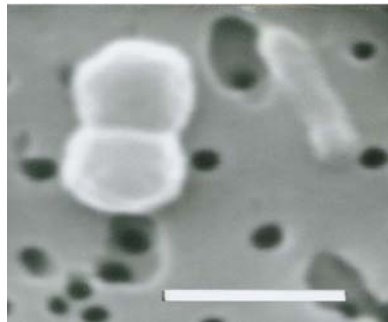


**Figure 3.** Photomicrograph showing a picocyanobacterium cell undergoing division (left) and bacterium (right), which was taken with scanning electron microscope (SEM). The image magnification (18,300) was captured with a scale bar of 1  $\mu\text{m}$  (Callieri and Stockner, 2002).

## 1.6 Autotrophic picoplankton (APP)

Picocyanobacteria form a major part of the autotrophic picoplankton (APP) and contribute significantly to the primary production especially in oligotrophic ecosystems. For many protists and small invertebrates, picocyanobacteria serve as an essential food source (Moser *et al.*, 2009). The APP plays a major role in the complex microbial food web particularly by channeling carbon to protozoa; hence, to higher trophic levels in the zooplankton (Callieri and Stockner, 2002). Heterotrophic (including mixotrophic) nanoflagellates and small ciliates are considered the major grazers of the picophytoplakton. It has been shown that among protozoa in oligotrophic lakes, about 90% of the grazing of picophytoplankton and bacteria are attributed to heterotrophic nanoflagellates (HNF); however, ciliates are only responsible for 10%. In suspension, *Vorticella aquadulcis*, *Halteria grandinella*, *Cyclidium* sp. and *Strobilidium hexachinetum* are active grazers among protozoa (Figure 4; A & B). Also, *Daphnia*, *Bosmina*, *Eubosmina*, and *Ceriodaphnia*, arthropods of the cladoceran genera, were observed to ingest picocyanobacteria (Figure 4; A). APP has the ability of contributing up to 65% of the primary production in mesotrophic and oligotrophic lakes (Becker *et al.*, 2002). In oligotrophic waters, 50-70% of fixed carbon is contributed by organisms that pass through filters of pore size 1  $\mu\text{m}$  to 2  $\mu\text{m}$  (Caron *et al.*, 1985). As well, the primary production of certain oceanic areas accounts for up to 80% (Li *et al.*, 1983).

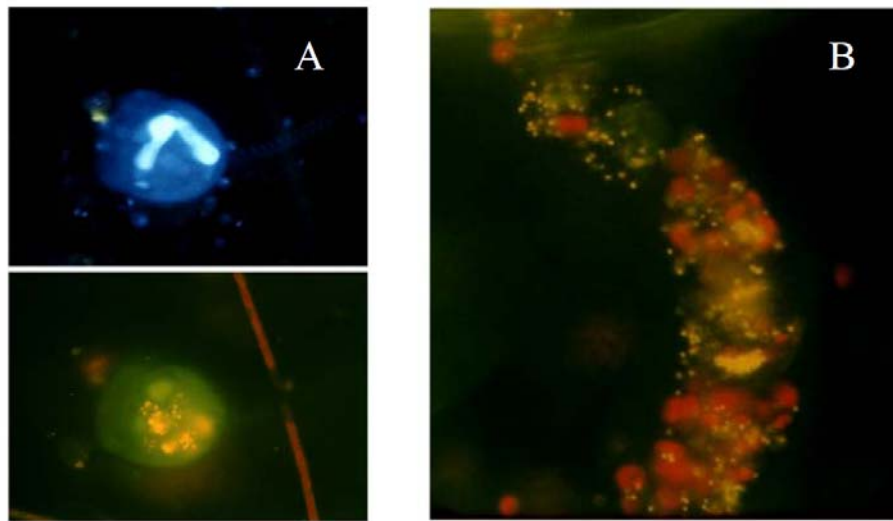


**Figure 4.** Epifluorescence microscopy image with 787.7x magnification showing *Vorticella* sp.; A, colored with DAPI under UV where the nucleus is clearly noticeable; B, blue excitation used to view the vacuoles which are full of picocyanobacteria (yellow). C, picocyanobacteria passing in the *Daphnia* gut viewed by epifluorescence microscopy (787.5x) (Callieri, 2007).

### 1.7 Single-cell picocyanobacteria

Three main genera of single-cell picocyanobacteria were defined including *Cyanobium*, *Synechococcus* and *Cyanothece diana/cedrorum*-type (Callieri and Stockner, 2002). *Synechococcus* and *Cyanobium gracile*, at the genus level, are cosmopolitan residents of nonmarine ecosystem (Crosbie *et al.*, 2003; Moser *et al.*, 2009). Callieri *et al.* (2007) suggests that, in fresh waters, *Synechococcus* and *Cyanobium* are the dominant genera of the prokaryotic picophytoplankton. *Cyanobium* morphology is spherical to oval cell (1-2  $\mu\text{m}$  long and 1  $\mu\text{m}$  wide) (Callieri and Stockner, 2002). It has been recently shown by Jezberová and Komárková (2007) that microcolony formed by



single cells of *Cyanobium* induced the grazing of the nanoflagellate, *Ochromonas* sp. DS. Interestingly, *Cyanobium* cells aggregated into microcolonies in the presence of protists developed spinae which is 1  $\mu\text{m}$  long tubes on the cell surface. Callieri *et al.* (2007) interpreted this behavior as defensive mechanism against predators; however, it is unknown yet if the spinae is species-specific or related to microcolony formation.

The first study conducted to investigate the temporal abundance and spatial distribution of *Synechococcus* was by Bailey-Watts *et al.* (1986) (Callieri, 2007). *Synechococcus* is rod-shaped (3-15  $\mu\text{m}$  long and 1-3  $\mu\text{m}$  wide) (Callieri and Stockner, 2002). 16S rRNA sequence identity (98%) between *Cyanobium* and *Synechococcus* revealed that they are closely related (Crosbie *et al.*, 2003; Ernst *et al.*, 2003; Moser *et al.*, 2009). Marine *Synechococcus* and cyanobacteria growing in the shallower freshwater lakes contain monovinyl chlorophyll *a* as the major photosynthetic pigment and phycoerithrin with the blue shifted absorption maximum ( $A_{\text{max}} = 565\text{-}575$  nm) (Ting *et al.*, 2002). Phycoerythrobilin ( $A_{\text{max}} = \approx 550$  nm), and phycoeuobilin ( $A_{\text{max}} = \approx 490$  nm) are the main chromophores present in *Synechococcus* sp. (Stockner *et al.*, 2000). Recently, Callieri *et al.* (2007) showed that picocyanobacteria located near the surface and at the deeper edge of the photic zone, water layer exposed to sufficient sunlight, from Lake Maggiore in Northern Italy have different photosynthetic efficiencies. However, fingerprinting analysis by denaturing gradient gel electrophoresis (DGGE) showed no particular genetic diversity. The shallower layers of the oligotrophic lakes showed higher density of cells which were more photosynthetically active and smaller than deeper cells. The DGGE was similar to the group B of the subalpine cluster I in Crosbie *et al.* (2003a). This study showed not only the first depth-dependant genetic diversity of

*Synechococcus*, but also a correlation to some physiological features (Callieri *et al.*, 2007).

In 1988, a new group of oceanic picophytoplankton including free living cells of the Prochlorophyta group was discovered with the new advances in flow cytometry (Chisholm *et al.*, 1988). The main light harvesting pigment include divinyl chlorophyll *a* (chl-*a*<sub>2</sub>) which are accompanied by divinyl chlorophyll *b* (chl-*b*<sub>2</sub>), zeaxanthin, alfa-carotene and a chlorophyll-*c*-like pigment as similar pigments of their putative ancestors. *Prochlorococcus marinus* coccoids are smaller than coccoid cyanobacteria. This strain is abundantly found in the North Atlantic, tropical and subtropical Pacific, Mediterranean, and Red Sea. In eutrophic lakes, only single filamentous forms were described in literature. Also, PC-rich Cyanobacteria or *Chlorella*-like eukaryotic cells prochlorophytes were also encountered in fresh water (Callieri, 2007).

Both marine *Synechococcus* and *Prochlorococcus* and freshwater *Synechococcus* and *Cyanobium* species form a separate bootstrap-supported “picocyanobacterial clade” from all other cyanobacterial radiations. The APP of freshwater, marine, and brackish ecosystems is dominated with the above groups (Crosbie *et al.*, 2003a; Ernst *et al.*, 2003; Urbach *et al.*, 1998). Six to seven clusters of picocyanobacteria have been shown to be within the picocyanobacterial clade of *sensu* Urbach *et al.* (1998) (Figure 5) (Callieri, 2007; Crosbie *et al.*, 2003a). Callieri (2007) has stated that our understanding of picocyanobacterial taxonomy is still in the beginning. For instance, although the marine *Synechococcus* of the subcluster 5.2 (Crosbie *et al.*, 2003a) are a sister-group to the form-genus *Cyanobium* of the Subalpine Subcluster II (Everroad and Wood, 2006), it do not possess the PE and are

halotolerant (Callieri, 2007). Thus, the type of pigment alone generally does not define a clade (Everroad and Wood, 2006).

In summary, the marine and freshwater APP consist of cyanobacteria which are less than 3  $\mu\text{m}$  in size. Primary production is attributed mainly to APP. PE-rich fresh *Synechococcus* is predominantly found in oligotrophic lakes as the major APP. However, both PE-rich marine *Synechococcus* strains and chlorophyll (Chl) *b*-containing *Prochlorococcus* coexist in oceanic water bodies (Ivanikova *et al.*, 2007).

### **1.8 Colonial picocyanobacteria**

Since we have discussed previously single-celled picocyanobacteria, it is noteworthy mentioning the main genera of species of common colonial picocyanobacteria found in freshwater which include *Aphanocapsa*, *Aphanothece*, *Chroococcus*, *Coelosphaerium*, *Cyanodictyon*, *Merismopedia*, *Snowella*, and *Tetrarcus* (Callieri and Stockner, 2002). The excretion of photosynthate-rich mucilage is one possible mechanism facilitating microcolony formation. Microcolonies has been observed in late summer under nutrient deficiency conditions in typical lakes (Callieri, 2007). It has been proposed that microcolony formation is a strategy for better nutrient recycling; however, it is not possible because the external mucilage hinders the uptake of nutrients in cells inside the microcolony. It is shown that active photosynthesis during severe nutrient deficiency result in the formation of photosynthate-rich mucilage (Callieri, 2007; Crosbie *et al.*, 2003b). Callieri and Passoni (2001) suggest that microcolonies initiated from single cells though the process of microcolony formation is not well understood (Callieri, 2007).

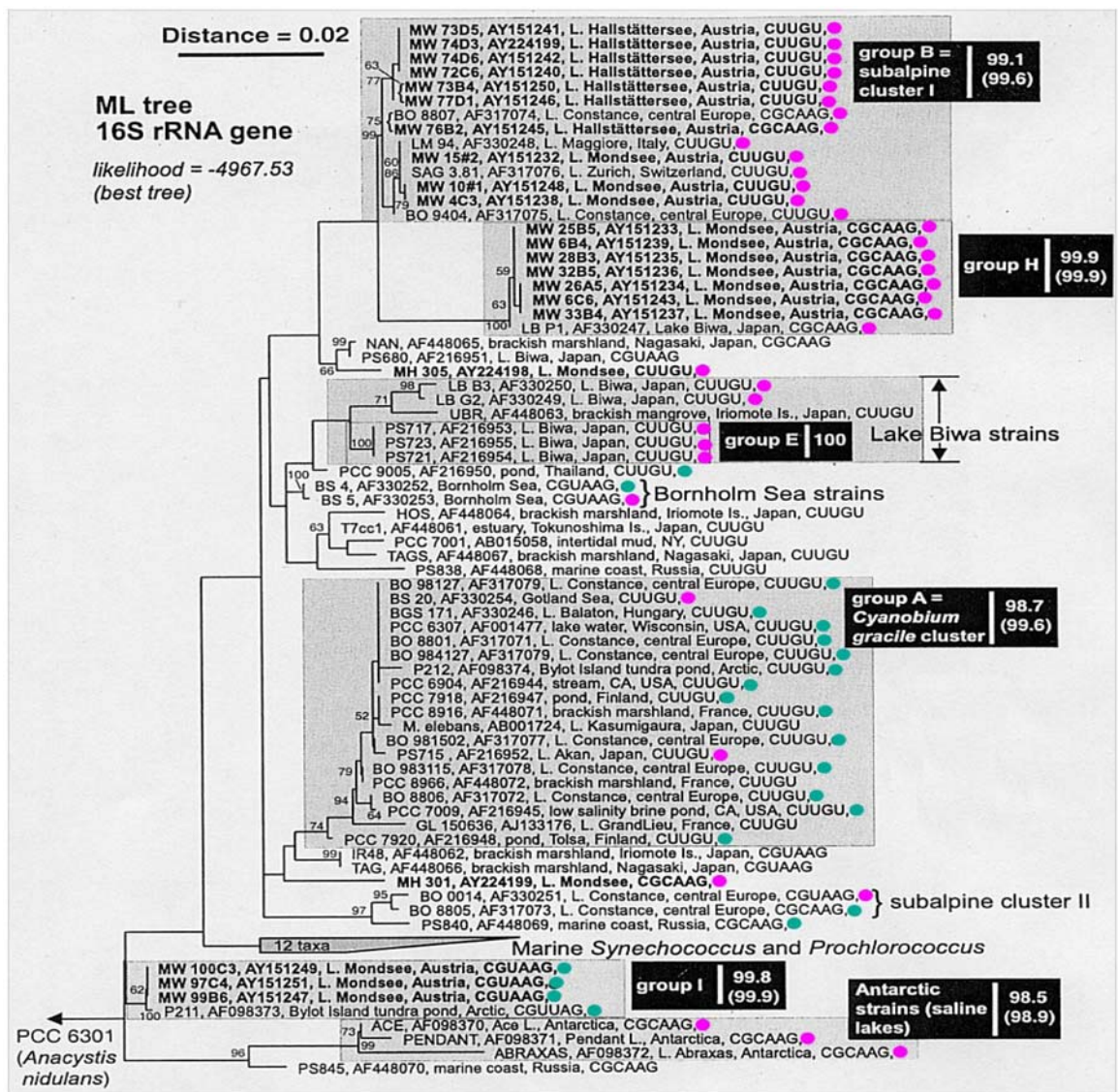


**Figure 5.** Phylogenetic tree representing the maximum likelihood of the picophytoplankton clade sensu Urbach *et al.* (1998) inferred from the 16S rRNA sequences (1,383 nt positions). Each isolate and Genbank accession numbers are shown at the terminal branches. Only Bootstrap values > 50% are displayed. On the right hand side of each group, minimum and mean (parentheses) pairwise percent similarities are displayed. Phycocyanin (PC) and phycoerythrin (PE) strains are represented respectively by green and pink circles. This tree is reproduced by Crosbie *et al.* (2003a) and adopted from Callieri (2007).

## 1.9 APP dynamics

Basin morphometry, thermal stratification, wind mixing, and nutrient fluctuations are factors that affect the complex variability of community structure. The variability of environmental factors makes the fittest adaptable species during a specific fluctuating phase dominate other available species. In large and deep lakes, the picophytoplankton peaks in a bimodal pattern observed in spring or early summer and autumn. It has been shown that picophytoplankton in Lake Maggiore reached maximum concentration at an optimum temperature of 18–20°C and at a depth of the thermocline, layer of water that separates the upper mixing surface water and calm water in the depth (Callieri, 2007). Among the picophytoplankton, picocyanobacteria and picoeukaryotes predominate other phytoplankton due to their smaller size which allows them to grow at low irradiance during the isothermal mixing in the spring. Furthermore, this period is accompanied with increase in the nano- and microzooplankton and limited nutrients which contribute to this decline during spring (Callieri and Stockner, 2002). Vertical abundance in the distribution of the picophytoplankton in several lakes has been observed including lower metalimnion (thermocline layer) and upper hypolimnion (lower stratification layer) of Lake Huron (North America), Lake Michigan (North America), and Lake Stechlin (Germany), in the metalimnion of Lake Baikal (south of the Russian region of Siberia), Lake Constance (borders of Switzerland, Austria, and Germany), and Lake Maggiore (Italy), as well as in the epilimnion (top stratification layer) of Lake Biwa (Japan), Lake Alchichia (Mexico), and Lake Kinneret (Israel).

In shallow and clear oligotrophic lakes, mainly present in mountains, the eukaryotic species dominate the almost negligible picophytoplankton (Callieri,

2007). Callieri *et al.* (2001) suggested that the high sensitivity of the APP to high light intensities and UV radiation explains their low abundance in shallow and clear lakes. Another possible explanation is the decrease in pH (<6) in mountain lakes which results in decreasing the number the picophytoplanktonic cells (Callieri and Stockner, 2002). On the other hand, in shallow, turbid, and eutrophic lakes, a high concentration of organic components protects the APP from high light intensities; therefore, present in these lakes at high concentrations. Also, shallow lakes which are intensely stained with humic matter, decomposed or partially decomposed organic material that floats on the surface, provide theoretically a suitable environment for picophytoplankton growth. Also, in humic lakes pH, nutrient availability (carbon, nitrogen, and phosphorous), penetrating light, and thermal stability all play a major role in the APP dynamics (Callieri, 2007).

Until 2006, phosphorous was considered the primarily limiting factor in the productivity of the picophytoplankton (Schindler, 2006). However, a recent study performed by Diaz *et al.* (2007) has demonstrated that nitrogen limitation even more than phosphorous affects APP productivity in ultraoligotrophic lakes of the Patagonian region of Argentina. Based on the Stockner model, the picophytoplanktons dominate other autotrophs proportionally when the lake and ocean conditions are more oligotrophic (Bell and Kalff, 2001). Callieri *et al.* (2007) stated that whether nitrogen or phosphorous are the ultimate nutritional limiting factors in both marine and lake ecosystem is currently open for debate.

## **1.10 Advances used in the classification of cyanobacteria**

The most favorable and appropriate methodology in understanding the picophytoplakton diversity includes the combination of both molecular and ecophysiological approaches (Callieri *et al.*, 2007). Advances in epifluorescence microscopy, flow cytometry, electron microscopy, and chromatographic analysis and immunofluorescence techniques are commonly used in the classification APP (Callieri and Stockner, 2002). Recently, quantitative real-time PCR (qPCR) is being used for assessing the biodiversity of environmental samples (Malinen *et al.*, 2003).

### **1.10.1 Epifluorescence and pigmentation**

In planktonic picocyanobacteria, pigmentation appears to be the major phenotypic difference. The major light harvesting pigments are manifested in two types of cells including red PE-rich and green PC-rich picocyanobacteria (Moser *et al.*, 2009). The phototrophic pigment can be detected by epifluorescence microscopy, a method described by several studies using various fluorochrome stains including acridine orange [AO], 3-6-diaminoacridine hemisulfate [proflavine], and fluorescein isothiocyanate [FITC] which makes the heterotrophic picoplankton visible. In contrast, phototrophic picoplankton autofluoresces which enables the discrimination of such organisms by epifluorescence (Caron, 1983). Blue and red excitation is used to observe picocyanobacteria as a function of photosynthetic pigment. Two types of cells are found including phycoerythrin (PE) cells and phycocyanin (PC) cells which produce yellow and dark red autofluorescence respectively (Figure 6) (Callieri and Stockner, 2002). Picoeukaryotes appear

red due to the presence of chlorophyll-*a* fluorescence; however, picocyanobacteria fluoresce depending on the presence and absence of phycobiliprotein and phycoerythrin phycobiliproteins (Callieri, 2007). Phycobiliproteins are pigments which are particularly present in blue-green algae, red algae, and some of the *Cryptomonadineae* family (Czeczuga, 1985).

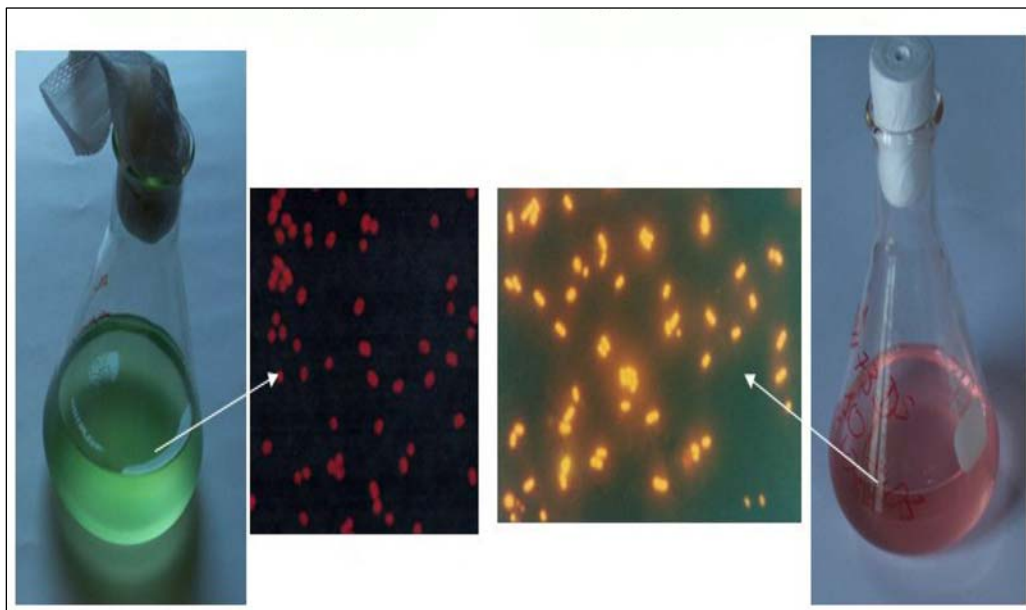


**Figure 6.** Cultures of *Synechococcus* sp. **A**, contain phycocyanin phycobiliprotein and lack phycoerythrin; **B**, phycoerythrin phycobiliprotein and lack phycocyanin. All microscopic images were obtained with blue excitation and magnified at 1250x with Zeiss AXIOPLAN epifluorescence microscope (Callieri, 2007).



### 1.10.2 Quantitative real-time PCR (qPCR)

Real-time PCR is based on the continuous detection of fluorescence during the PCR run in which quantification occurs during the exponential phase of amplification. Conventional PCR methods are end-point detection PCR which depend on resolving agarose gels. Bias of end-point detection is avoided in the exponential phase because all reagents are fresh and available (Malinen *et al.*, 2003). At the exponential phase, the reaction is highly precise and specific since the exact doubling amplicon is accumulating every cycle. The accumulation of the PCR amplicon is continuously monitored during PCR cycles at the exponential phase (Applied Biosystems). In the *TaqMan* assay, fluorescence detection is performed during PCR when the *Taq* DNA polymerase cleaves the dual-labeled (fluorophore and quencher) fluorescent hybridization probe which gets integrated inside the amplified region during primer extension (Malinen *et al.*, 2003). SYBR Green I (SG) is also being used in the quantification of double-stranded (ds) DNA of crude extracts of environmental samples. Although SG possesses favorable photophysical properties including temperature stability, selectivity for double stranded DNA and high sensitivity, it includes unmarked sequence non-specificity. SG intercalates DNA during primer extension that gives fluorescence when bound to the dsDNA; however, it is normally non-fluorescent in the unbound state (Malinen *et al.*, 2003).

Furukawa *et al.* (2006) developed specific quantitative real-time PCR (qPCR) using SG fluorescent dye to quantify microcystin-producing cyanobacteria in lake water samples which is based on Microcystin Synthetase A (*mcyA*) gene. Also, qPCR was used in quantification of hepatotoxin nodularin-producing *Nodularia* in the Baltic Sea. The primers

used were specific to the subunit F of the nodularin synthetase gene (*ndaF*) (Koskenniemi *et al.*, 2007). In the former study, standard curve was developed as a correlation of predetermined cell concentration, established by serial dilutions of extracted genomic DNA of equivalent number of specific cells, in relation to the cycle threshold (Ct) values of the diluted DNA. Number of cells was determined by direct microscopy (Furukawa *et al.*, 2006). The latter study used different approach to establish the standard curve which was also determined as a correlation of gene copy numbers and Ct. Specific formula, described later in this study, was used to calculate the gene copy number per  $\mu\text{L}$ . Ten-fold serial dilutions of DNA copy numbers per 10  $\mu\text{L}$  of qPCR reaction were used to make the standard curve. Since this study aims to quantify specific cells of nodularin toxin-producers, DNA of standard curve was extracted from specific strains of nodularin-producing *Nodularia* (Koskenniemi *et al.*, 2007). Recently, community structure in seven English post-glaciation and artificial lakes were assessed by Sánchez-Baracaldo *et al.* (2008). TaqMan PCR assay was used by targeting clones of specific 16S rRNA sequences which were used as standards in the qPCR. The previous studies were briefly described to offer an overview of approaches used in establishing qPCR standard curve as a crucial aspect of this study.

### **1.11 Lake Superior as a model of ultraoligotrophic lake**

Lake Superior has the largest surface area (82,413 km<sup>2</sup>) among freshwater lakes in the world and belongs to the Laurentian Great Lakes located in North America (Canadian and U.S borders). The Laurentian Great Lakes forms 20% of the world's lacustrine freshwater (Ivanikova *et al.*, 2007). After Lake Baikal, located in southern Siberia, Lake Superior is the second largest in volume which contains about 10% of the world's surfacial fresh water. The

geology and geomorphology of the lake drainage area result in the oligotrophic nature and chemical stability of the lake. The ancient (2500-3000 billion years old) crystalline shield with chemically stable igneous (formed by magma) and metamorphic rocks forms almost the entire drainage basin of Lake Superior (Ivanikova, 2006; Weiler, 1978). The chemical composition of Lake Superior water is close to rainwater due to several reasons. About 50% of the water falling into the terrestrial watershed evaporates. The rest of the water is transferred to the lake readily through numerous trajectories, therefore only very limited amount of minerals are able to dissolve in the running water. Furthermore, it was noticed that a significant amount of the basin water comes in contact directly with the lake water which is subjected to dilution of the dissolved salts. Iron and phosphorous are extremely limited in Lake Superior. Moreover, light and temperature systems are unfavorable for photosynthesis (Ivanikova *et al.*, 2007). The area surrounding the lake is mostly covered with forests and a thinly populated area with minimal agricultural activity (Ivanikova, 2006; Matheson and Munawar, 1978). One study followed the concentration of the major ions and nutrients (calcium, magnesium, chloride, sodium, potassium, phosphate, sulfate and silica) over a period of 100 years and found that they were constant (Weiler, 1978). Lake Superior is considered ultraoligotrophic compared to other Laurentian Great Lakes and a number of European lakes in which the phytoplankton biomass is extremely low (Matheson and Munawar, 1978).

Ivanikova *et al.* (2007) indicated that despite the importance of APP in Lake Superior which contribute to 50% of the total chlorophyll in the open lake, little is known about the diversity of the APP in this ecosystem. Matheson and Munawar (1978) have studied the species diversity in Lake Superior. This study showed that Lake Superior includes a high species diversity including

285 taxa. The predominant group found in Lake Superior consisted of diatoms which accounted for 31% of the total number of species identified. Chlorophytes (22%), chrysomonads (20%), cyanobacteria (12%), cryptomonads (8%) and dinoflagellates (6%) were also found to populate Lake Superior. *Cyclotella stelligera* and *C.comta*, indicators of oligotrophic conditions, were the most dominant diatoms in Lake Superior. Among cyanobacteria species, filamentous forms, which are colonial picoplankton, were found to be dominant including *Oscillatoria limnetica*, *Oscillatoria sp.*, *O. minima*, *Lyngbya sp.*, *L. limnetica*, *Anabaena pulchra*, and *Anabaena sp.* Also, *Aphanothece*, *Aphanocapsa*, *Chroococcus*, and *Merismopedia sp.* were also identified. No unicellular *Synechococcus*-like picocyanobacteria were reported by Matheson and Munawar (1978). However, Fahnensteil *et al.* (1986) indicated the presence of picoplankton (< 3 µm cells) in Lake Superior including eukaryotic flagellates, non motile eukaryotic cells, and chroococcoid cyanobacteria. About 20% of the total primary production is contributed by chroococcoid cyanobacteria with orange autofluorescence, an indication of PE-rich cells. These cells were present at both epilimnion and hypolimnion of Lake Superior in September 1983. Lake Superior, as described earlier, is an ultraoligotrophic lake and is least disturbed by human activities, which suggests that picophytoplankton might be highly preserved in such an ecosystem (Weiler, 1978; Munawar and Munawar, 1978).

### **1.12 *Synechococcus sp.* and novel Lake Superior cluster I (LSI) and II (LSII)**

The small size and morphological similarity of *Synechococcus*-like cells makes their classification difficult with conventional microscopic techniques (Postius and Ernst, 1999). Moreover, the true distribution of APP is

underestimated by traditional cultivation techniques which are biased towards larger phytoplankton and PC-rich cyanobacteria (Ivanikova *et al.*, 2007). Currently, *Synechococcus* is not considered to be monophyletic and was classified on the basis of the G and C content of DNA, type of habitat (Waterbury and Rippka, 1989), type of pigment, 16S rRNA, and *cpcAB* (Garcia-Pichel *et al.*, 1998; Urbach *et al.*, 1998; Ivanikova *et al.*, 2007). To date, all the isolated *Synechococcus*-like and *Prochlorococcus* picocyanobacteria clustered within the “picocyanobacterial clade” mentioned earlier (Urbach *et al.*, 1998; Callier, 2007; Crosbie *et al.*, 2003a; Ernst *et al.*, 2003). Moreover, high bootstrap values are also retained in picocyanobacterial phylogenetic trees when studying the *cpcAB* and the 16S-23S rRNA IGS (Ernst *et al.*, 2003; Robertson *et al.*, 2001).

Our study is based on novel findings by Ivanikova *et al.* (2007). The phylogenetic diversity of Lake Superior APP was characterized by sequences of the 16S rRNA and *cpcBA* IGS. Samples were collected from different locations at the western arm of Lake Superior during two cruises (Figure 10). In May 2004 during spring isothermal mixing, samples were collected from a depth of 5 m including Sterner B (SB), Castle Danger 1 (CD1), and Western Mid-lake (WM). In September 2004, samples were collected from the epilimnion and deep chlorophyll maximum (DCM) from CD1, WM, SB, and near shore Portage Deep (PD) stations (Figure 10). Libraries were constructed by inserting PCR amplicons of the 16S rRNA and *cpcBA* IGS followed by high throughput sequencing. Phylogenetic analysis of the CD1 library of samples collected at the epilimnion (5 m depth) showed that out of the 32 unique sequences, thirty-one were found to cluster within the picocyanobacterial clade sensu Urbach *et al.* (1998) with 99% bootstrap support. Interestingly, most of the sequences clustered with two novel groups

including Lake Superior Cluster I (LSI) and Cluster II (LSII). Average pairwise sequence similarities between LSI and LSII are 99.4% and 99.7% respectively. LSI and LSII formed two novel independent clusters which are not found in any freshwater APP strains isolated earlier (Figure 8). The novel clusters are closely related to each other and Crosbie group H which includes a number of PE-rich isolates from Lake Mondsee, Austria, and a PE-rich strain (LPB1) isolated from Lake Biwa, Japan (Crosbie *et al.*, 2003a; Ivanikova *et al.*, 2007). Only three sequences did not cluster within LSI and LSII. LSI and LSII were found at the epilimnion and DCM of CD1. September epilimnion samples including WM and SB and DCM library from WM showed that LSI and LSII are major clusters as well. However, in WM DCM libraries fewer sequences clustered within LSI compared to the September epilimnion samples. Libraries constructed in May (2004) also showed sequences from LSI and LSII. However, less cyanobacterial sequences were obtained in May compared to those collected in September (2004). Only 4% of sequences obtained from PD showed the presence of LSI and LSII. Also, PD-specific sequences were found (PDI and PDII) which did not cluster with any previous cyanobacterial isolates. Interestingly, PD shows high genetic diversity of isolates including MH305, Crosbie group H, the Lake Biwa cluster, and new and specific PD cluster I (PDI) and (PDII) II. It is noteworthy that LSI and LSII novel clusters were not isolated into cultures, although their phylogenetic assembly suggests that they are PE-rich picocyanobacteria (Ivanikova *et al.*, 2007).

Flow cytometry analysis showed that PE-rich picocyanobacteria dominates the APP. However, APP shows a significant shift from late winter to summer. Picoeukaryotes, PC-rich and PE-rich picocyanobacteria are present

in winter to early spring. In summer, PE-rich picocyanobacteria are solely present (Figure 7).

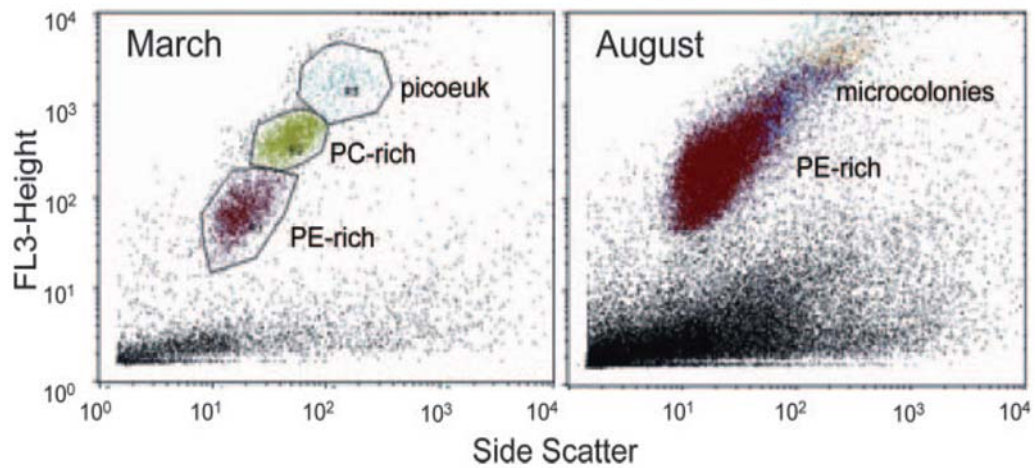


**Figure 7.** Flow cytometry of water samples collected from CD1 during late winter (March) and summer (August), 2006. Pigment fluorescence of APP is shown on the plots including PE-rich APP, PC-rich APP, picoeukaryotes, and PE-rich microcolonies (Ivanikova *et al.*, 2007).

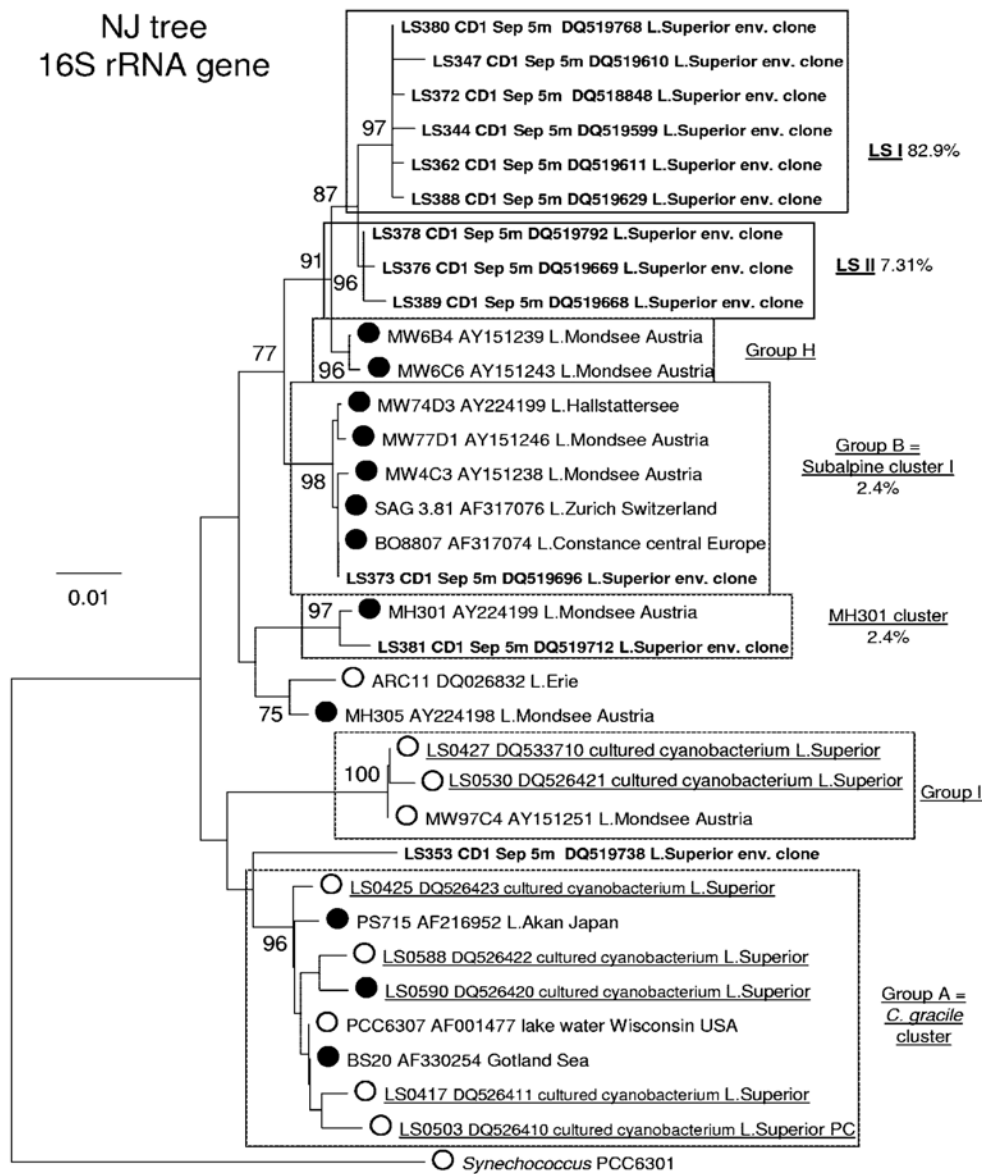


**Figure 8.** Phylogenetic tree inferred from the 615 bases of the 16S rRNA sequences from samples collected at CD1 station. In the 16S rRNA gene neighbor-joining (NJ) tree, the major clusters of picocyanobacteria described previously are shown with outgroup strain *Synechococcus* PCC 6301. PE-rich and PC-rich cells are represented in bold circles and white circles respectively. Percentages of each cluster in the 16S rRNA library are shown on the right terminal branches. Bootstrap values (numbers at nodes) < 70% are not shown (Ivanikova *et al.*, 2007).



### **1.13 Specific quantitative real-time PCR (qPCR) of Lake Superior Cluster I (LSI)**

It is valuable to investigate the dominant and the highly adaptable picocyanobacteria group in Lake Superior as they are major contributors in the food chain. Also, since picocyanobacteria are phototrophic organisms and Lake Superior has a large surface area, these organisms are ecologically important in combating global warming.

In this study, we quantified the *Synechococcus* strains that cluster within LSI present in Lake Superior with specific quantitative real-time PCR. Our approach included the development of two standard curves, one that covers general picocyanobacteria (picos) and another that specifically covers LSI. Since this group has not been isolated into cultures and therefore no genomic DNA is available, we have circumvented the problem by cloning a specific sequence of the 16S rRNA into a vector which was successfully transformed into *E.coli* competent cells followed by culturing and subsequent isolation. Eventually, standards prepared by serial dilutions of plasmid DNA were used to build our standard curves. The generated qPCR protocol can be used to monitor the dynamics of picos and LSI in different seasons of the year. Moreover, other primers can be generated to quantify all groups isolated from Lake Superior.

## *Chapter II*

### **MATERIALS AND METHODS**

#### **2.1 Sample collection**

All samples were collected from the western arm of Lake Superior in a research cruise during September 2004 (Figure 9) by Dr. George Bullerjahn of the Department of Biological Sciences, Bowling Green State University. The method of collection is described in details by Ivanikova *et al.* (2007). When water columns are stratified in September 2004, water samples were collected from Sterner B (SB; 46.8°N, 92.13°W, Depth 5 m), Castle Danger 1 (CD1; 47.30°N, 91.67°W, Depth 5 m), Western Mid-lake (WM; 47.33°N, 89.90°W, Depth 30 m), and nearshore Keweenaw Waterway station Portage Deep (PD; 47.06°N, 88.50°W, Depth 7 m). The collected water from all stations was filtered (450 mL except for SB; 1500 mL) through 0.45- $\mu$ m polycarbonate filters which were subsequently placed in TE buffer (10 mM Tris-HCl [pH.7.5], 1 mM EDTA-Na<sub>2</sub>) stored at – 20 °C. For cyanobacterial samples to be shipped to Lebanon, cells were lyophilized and then stored after arrival at – 80 °C for DNA extraction.

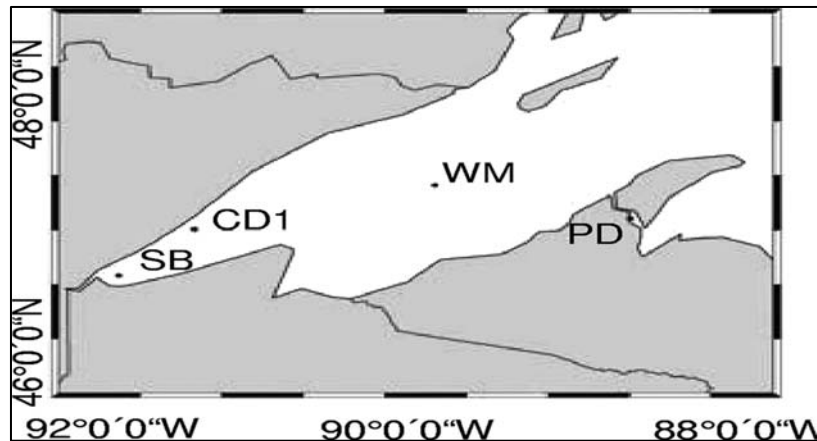


**Figure 9.** Map of the western arm of Lake Superior showing hydrographic locations where samples were collected (Ivanikova *et al.*, 2007).

## 2.2 Genomic DNA extraction

The protocol for Gram-positive bacteria of the DNeasy Blood & Tissue Kit (Qiagen) was used for extracting genomic DNA. STET buffer (50 mM Tris-HCl, 50 mM sodium EDTA, 5% Triton X-100, 8% sucrose, lysozyme 10 mg/mL) was used instead of the enzymatic lysis buffer described in the kit. The STET buffer was adjusted to a pH of 8 before adding lysozyme. Finally, the yield and absorption ratio 260/280 nm of the extracted DNA were determined with NanoDrop spectrometer (Thermo Scientific).

## 2.3 PCR Amplification

PCR was used to amplify specific DNA sequences of the 16S rRNA gene in a 20  $\mu$ L reaction.

### 2.3.1 Primer

The primers used in this study are CYA 107F (5'-GACGGGTGAGTAACGCGTG-3'), PICO 224R (5'-ACGCGAGCTCATCCTCAGG-3'), LSI 258R (5'-TGGTAAGCCATTACCTTACCAAC-3'), and LSI 261R (5'-CTTGGTAAGCCATTACCTTACC-3'). All primers were designed by Dr. Irina Ilikchyan at the University of California, Santa Cruz. LSI 261R and LSI 258R primers are specific for LSI isolates. PICO 224R is a general primer for all picos. CYA 107F was used in all PCR reactions. The following combination of primers were used separately in all the reactions performed in this study (CYA 107F + PICO 224R, CYA 107F + LSI 258R, and CYA 107F + LSI 261R). Target amplicons are 118 bp, 152 bp, 154 bp in length, respectively.

### 2.3.2 PCR conditions and reagents

The reaction included 0.2 mM of dNTPs, 1X of Taq buffer, 2.5 mM MgCl<sub>2</sub>, 0.4 μM of each primer, 50 ng of template DNA and 0.1 U/μL of AmpliTaq Gold (Roche). Initially, the reaction mixture was held at 95 °C for 2 min followed by 35 cycles of denaturation at 95 °C for 30 s, annealing at 55 °C for 30 s, and extension at 72 °C for 15 s. Final extension at 72 °C for 10 min and samples were left at final hold for infinity at 4 °C. The PCR products were viewed by performing 1% agarose gel electrophoresis at 100 V. All gels were prepared with 1x TAE containing 4 μg/mL ethidium bromide and visualized with UV imaging systems.

## **2.4 Cloning Procedures**

### **2.4.1 PCR**

Genomic DNA of CD1 sample was amplified by PCR in 50  $\mu$ L reaction using CYA 107F and LSI 258R primers and the PCR insert was created to be used for building the standard curve for quantifying general picocyanobacteria (picos). PCR products were viewed by performing 1% agarose gel electrophoresis at 100 V (all PCR conditions and gel specifications were described previously). The same reaction was performed with CYA 107F and LSI 261R and specific PCR insert was created for building the specific standard curve covering Lake Superior Cluster I (LSI).

### **2.4.2 DNA purification from agarose gel**

Bands were viewed under UV light and excised sharply from the agarose gel. DNA was purified as described in QIAquick Gel Extraction Kit using microcentrifuge protocol (Qiagen).

### **2.4.3 Cloning reactions**

Cloning reactions and transformation procedures were followed as described in TOPO TA Cloning Kit (Invitrogen). TOP10 competent cells were used as received (Invitrogen).

#### **2.4.4 Screening for transformants**

From each transformation reaction, cells (10-50  $\mu$ L) were spread on a prewarmed ampicilline (Amp) selective Luria-Bertani (LB) plate and incubated overnight at 37 °C. The recipe of LB plates is described in TOPO TA Cloning Kit (Invitrogen). Two to three white colonies were sub-cultured several times. Cryobanks were also created and stored in duplicates at – 20 °C and – 80 °C.

#### **2.4.5 Plasmid DNA Extraction**

Plasmid DNA was extracted from 2 to 3 white colonies as described in QIAprep Spin Miniprep Kit using microcentrifuge protocol (Qiagen). DNA yield and 260/280 nm were determined as described previously.

#### **2.4.6 Amplification of the ligated PCR insert**

The PCR step described previously (2.3.1 PCR in cloning procedure) was followed to verify successful cloning.

#### **2.5 Sequencing**

Partial sequencing of the pCR 2.1-TOPO including the PCR insert was carried out.

### **2.5.1 Pre-sequencing PCR**

M13 Forward (5' GTAAAACGACGGCCAG 3') and M13 Reverse (5' CAGGAAACAGCTATGAC 3') are the primers (Invitrogen) used to amplify a portion of the construct including the PCR insert which was amplified initially with CYA 107F and LSI 261R. The PCR reaction (20  $\mu$ L) included 0.2 mM of dNTPs, 1X of Taq buffer, 2.5 mM MgCl<sub>2</sub>, 0.4  $\mu$ M of each primer, 50 ng of template DNA and 0.1 U/ $\mu$ L of AmpliTaq Gold (Roche) at 55 °C for 30 s and extension at 72 °C for 30 s and final extension at 72 °C for 10 min. The reaction was held at 4 °C for infinity. Amplicon size is 356 bp. Aliquots of samples (5  $\mu$ L) and 1 negative control were loaded to 1% agarose gel. The electrophoresis apparatus was fixed at 100 V, and the gel was left on a run for 30 min.

### **2.5.2 Purification (ExoSAP-IT, modified methodology)**

From the remaining PCR product, 10  $\mu$ L was transferred into a new PCR tube. The ExoSAP-IT (USB Corp., Cleveland, Ohio) was mixed by pipetting the solution up and down. ExoSAP-IT (4  $\mu$ L) was added and placed in the thermocycler under the following conditions: 30 min at 37 °C, and 15 min at 80 °C. All samples were left at a final hold for infinity at 20 °C.

### **2.5.3 Sequencing PCR**

The ABI Prism BigDye Terminator v3.1 Cycle Sequencing Kit (Applied Biosystems) was used for sequencing the amplicons. Two PCR tubes were prepared containing only one primer (2  $\mu$ M of the M13 Forward and M13 Reverse primers) in 10  $\mu$ L reaction. BigDye (4  $\mu$ L), and purified DNA (5  $\mu$ L)

were added to each PCR tube. The reaction was performed under the following conditions: 25 cycles at 96 °C for 10 s, 50 °C for 5 s, and 60 °C for 4 min. All reaction tubes were left at final hold for infinity at 20 °C.

### **2.5.3.1 DNA precipitation (Dye-Ex)**

DNA precipitation was performed by the DyeEx 2.0 Spin Protocol for Dye-Terminator Removal (QIAGEN).

### **2.5.3.2 Loading and Processing**

HIDI formamide (20 µL, Applied Biosystems) was used as a loading media, and the sample was vortexed while stopping every 2 s. The sample was collected at the bottom of the tube by performing a quick spin. Samples were loaded vertically to a different well in the sequencing plate. After closing the plate with septa, it was placed in the thermal cycler without closing the cover under the following conditions: 5 s at 95 °C, and 5 s at 4 °C. Samples were left at final hold for infinity at 4 °C. The plate was then processed for sequencing electrophoresis on an ABI 3130xl Genetic Analyzer (Applied Biosystems).

### **2.5.3.3 Data analysis**

Consensus sequence of both M13 Forward and Reverse primers was created by CLC Main Workbench 4.1.1 software.



## 2.6 Quantitative real-time PCR (qPCR)

The CYA 107F and PICO 224R primers were used to create standard curve to quantify picos of the cyanobacterial picoplankton and the CYA 107F and LSI 261R primers were used to create standard curve to specifically quantify LSI. qPCR protocol was developed using LightCycler instrument with LightCycler software version 3.5 (Roche). This reaction was performed in 20  $\mu$ L reaction including 3 mM MgCl<sub>2</sub>, 2  $\mu$ L of Reaction Mix (LightCycler FastStart DNA Master SYBR Green I; Roche), and 0.35  $\mu$ M of each primer. The amplification program consisted of the following steps: (i) preheating at 95 °C for 10 min, with a heating rate of 20 °C s<sup>-1</sup>; (ii) quantification, including 45 cycles (95 °C for 0 s, 55 °C for 5 s, and 72 °C for 8 s), fluorescence measurement at the end of each cycle at 72 °C through channel F1 (530 nm), and a heating rate of 20 °C s<sup>-1</sup>; and (iii) melting curve analysis, which included heating from 77 °C to 97 °C at rate of 0.1 °C s<sup>-1</sup> and fluorescence measurement continuously through channel F1 (530 nm)

A standard curve was developed as a correlation between the DNA copy numbers and the cycle threshold (Ct). The second derivative maximum was the analysis method used. This method offers high reproducibility and automatic data calculation excluding the user and background noise influence. Plasmid DNA extracted from the transformed *E.coli* cells was used to build the standard curve in serial dilutions of 10 folds of DNA copy numbers ( $2 \times 10^2$  to  $2 \times 10^6$  per 20  $\mu$ L of the reaction mix). Plasmid DNA containing PCR fragment amplified with CYA 107F and LSI 258R were used to build the standard curve, covering the general picos, by amplifying with CYA 107F and PICO 224R. On the other hand, plasmid DNA containing amplicon of

CYA 107F and LSI 261R was used to build the specific standard curve of LSI by amplifying with same primers used in creating the construct. The DNA copy number for standard curve were calculated using the following formula:  $[\text{DNA concentration (g } \mu\text{L}^{-1}) \times \text{Avogadro constant (6.022} \times 10^{23} \text{ copies mol}^{-1}) \times \text{sample volume (}\mu\text{L)}] [\text{vector molecular weight (g mol}^{-1})]^{-1} = \text{DNA copy numbers}$ .  $\text{MW} = \text{vector size (bp)} \times 660 \text{ Da/bp} = \text{Da (or g mol}^{-1})$  (Koskenniemi *et al.*, 2007; Roche, 2000). The vector size pCR 2.1-TOPO (Invitrogen) was used to calculate the vector molecular weight (vector size 3900 Da + PCR product 155 Da)  $\times 660 = 2.67 \times 10^6 \text{ Da}$ .

Gene copy numbers from water samples including community DNA of picoplankton organisms were calculated using the following formula:  $[\text{DNA concentration (g } \mu\text{L}^{-1}) \times \text{Avogadro constant (6.022} \times 10^{23} \text{ copies mol}^{-1}) \times \text{sample volume (}\mu\text{L)}] [\text{genome molecular weight (g mol}^{-1})]^{-1} = \text{DNA copy numbers}$ .  $\text{MW} = \text{genome size (bp)} \times 660 \text{ Da/bp} = \text{Da (or g mol}^{-1})$ . The genome size of *Synechococcus* sp. WH 8102 (NCBI accession number [NC\\_005070](#)) was used as a reference strain to calculate the genome molecular weight, and it was calculated as the following:  $2.4 \times 10^6 \text{ Da} \times 660 = 1.58 \times 10^{10} \text{ Da}$ . It is noteworthy that with each qPCR reaction three standards were included to minimize the error with the applied standard curve.

## Chapter III

### RESULTS

#### 3.1. LSI 261R primer sensitivity

The LSI 261R primer anneals to specific sequence (23 bp) of the 16S rRNA gene of Lake Superior Cluster I (LSI). LSI 261R primer showed high sensitivity even with low DNA concentrations (1 ng per 20  $\mu$ L of PCR reaction) (Figure 10). It is noteworthy that LSI 258R was initially used instead of LSI 261R; however, this primer showed low sensitivity for low DNA concentration (experimental results are not shown).

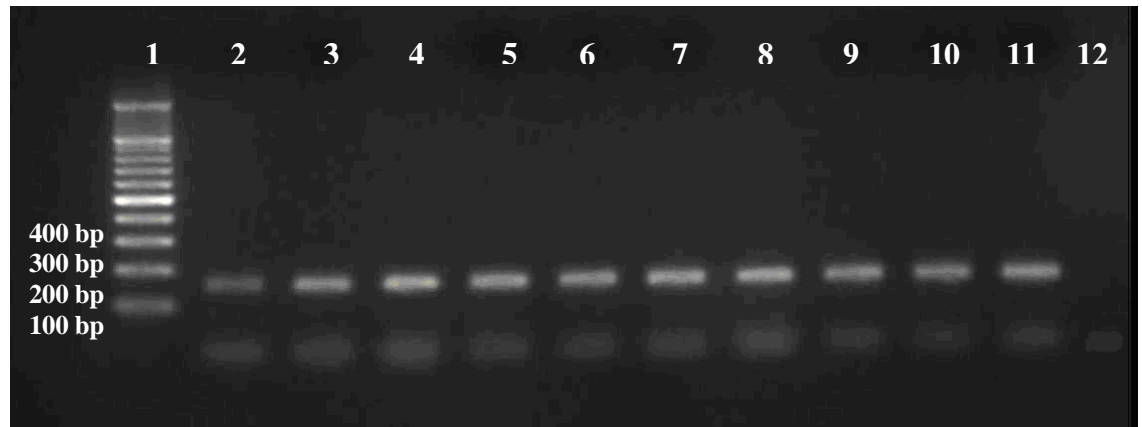


**Figure 10.** Amplification with CYA 107F and LSI 261R primers viewed by 1% agarose gel electrophoresis. Lane 1, contains 100 bp molecular ladder; Lane 2-11, serial dilutions of genomic DNA from sample collected from CD1 (1–10 ng per 20  $\mu$ L of PCR reaction) revealing high sensitivity of LSI 261R even with low DNA concentrations; Lane 12, no template control.

### 3.2 Cloning and sequencing gels

The efficiency of cloning of the TOPO TA Cloning Kit (Invitrogen) was tested by sequencing of the specific cloned sequence of LSI (Figures 11 & 12). Moreover, cloning of the specific 16S rRNA sequence of LSI was confirmed by PCR which was amplified with CYA 107F and LSI 261R (Figure 13). PCR amplicons with LSI 258R and CYA 107F contains a specific DNA sequence of the 16S rRNA gene that is found essentially in all picos. The reverse primer (PICO 224R) anneals specifically to this sequence. Therefore, serial dilutions of plasmid DNA from the described clones of PCR amplicons was amplified using CYA 107F and PICO 224R to generate the standard curve used for quantifying general picos. Again, successful cloning was confirmed with PCR (Figure 14).

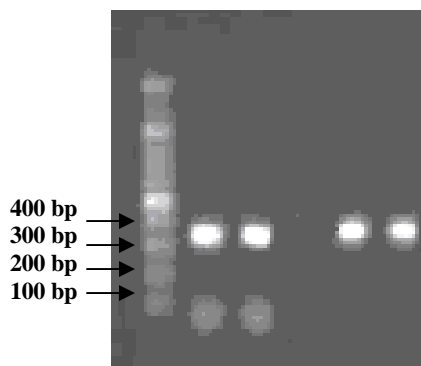


**Figure 11.** Pre-sequencing PCR with M13 Forward and M13 Reverse primers of cloning construct (including insert created by PICO 224F and LSI 261R primers) in lane 2, 3, 5, and 6 and the amplicon size is 356 bp. Lane 1, includes 100 bp molecular ladder; Lane 4, no template control.

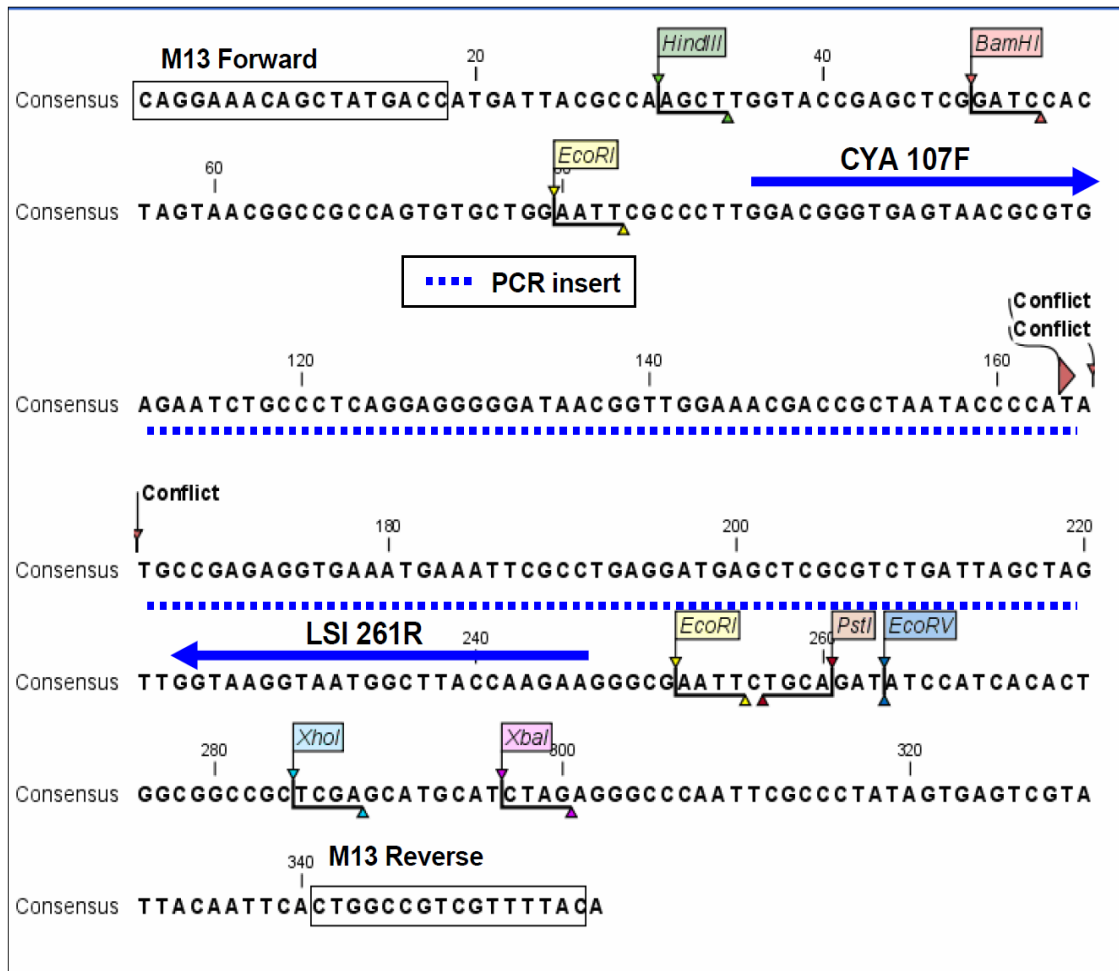


**Figure 12.** Consensus sequence of both M13 Forward and M13 Reverse primers created by CLC Main Workbench software showing successful cloning of the PCR insert with primers CYA 107F and LSI 261R. The underlined sequence represents the region of the 16S rRNA amplified where the annealing sequence of LSI 261R is highly specific for sequences that clusters with LSI. Conflict in sequence reflects a difference in the DNA sequence between the reverse and forward primer sequencing reactions of the same amplified fragment.

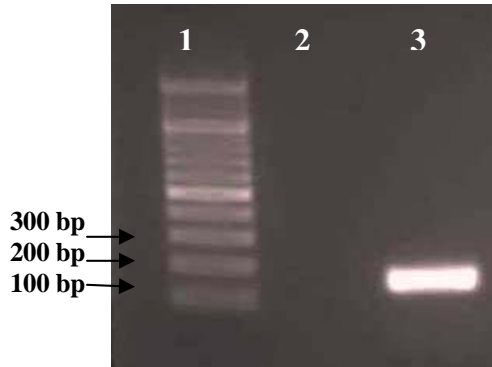


**Figure 13.** Amplification of plasmid DNA (20 ng) to confirm successful cloning procedure of LSI 16S rRNA sequence viewed by 1% agarose gel electrophoresis. Lane 1, contains 100 bp molecular ladder; Lane 2, No template control; Lane 3, 154 bp amplicon amplified with CYA 107F and LSI 261R.

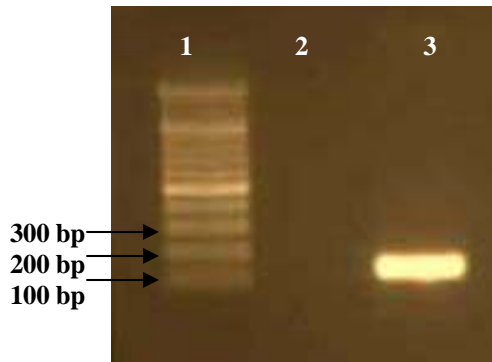


**Figure 14.** Amplification of plasmid DNA (50 ng) to confirm successful cloning used for building the standard curve of general picos viewed by 1% agarose gel electrophoresis. Lane 1, contains 100 bp molecular ladder; Lane 2, no template control; Lane 3, 150 bp amplified with CYA 107F and LSI 258R.

### **3.3 Specificities of general picos and LSI qPCR**

All amplification curves showed no DNA contamination which was inferred from no template control (Figures 15 & 19). Melting curve analysis included an evaluation of the melting curve data obtained by this study (Figure 17). The melting curve analysis showed no unspecific amplification or primer dimer for the specific LSI and general picos standard curve (Figure 18) and sample quantification (Figure 20). The concentration of picos and LSI from DNA samples were determined by evaluating the Ct values (Tables 2 & 3). The slope of standard curve represents the overall reaction efficiency and should be between -5.700 and -2.900. Slope values obtained from picos and LSI standard curves are -3.435 and -4.540 respectively showing good efficiency (Figure 16).

The pattern of melting peaks of LSI samples and standards indicated the presence of position nucleotide variation in the annealing sequence of LSI 261R (Figures 18; B & 20; B). We found that the pattern of melting peaks obtained by picos standards might be due to different DNA template concentrations. Separate real-time PCR with standards of high and low DNA concentrations was performed (Figure 21). Since the shift in melting temperature ( $T_m$ ) occurred only in standards of different DNA template concentrations and not with samples which contained the same DNA template concentrations, we have amplified DNA from samples and standards and they showed the same amplicons size (Figure 22). This showed that there was no unspecific amplification in the DNA sequence between standards and samples. Another possible explanation might be due to sequence variability in the PICO 224R annealing sequence which is discussed in detail in section 4.1.

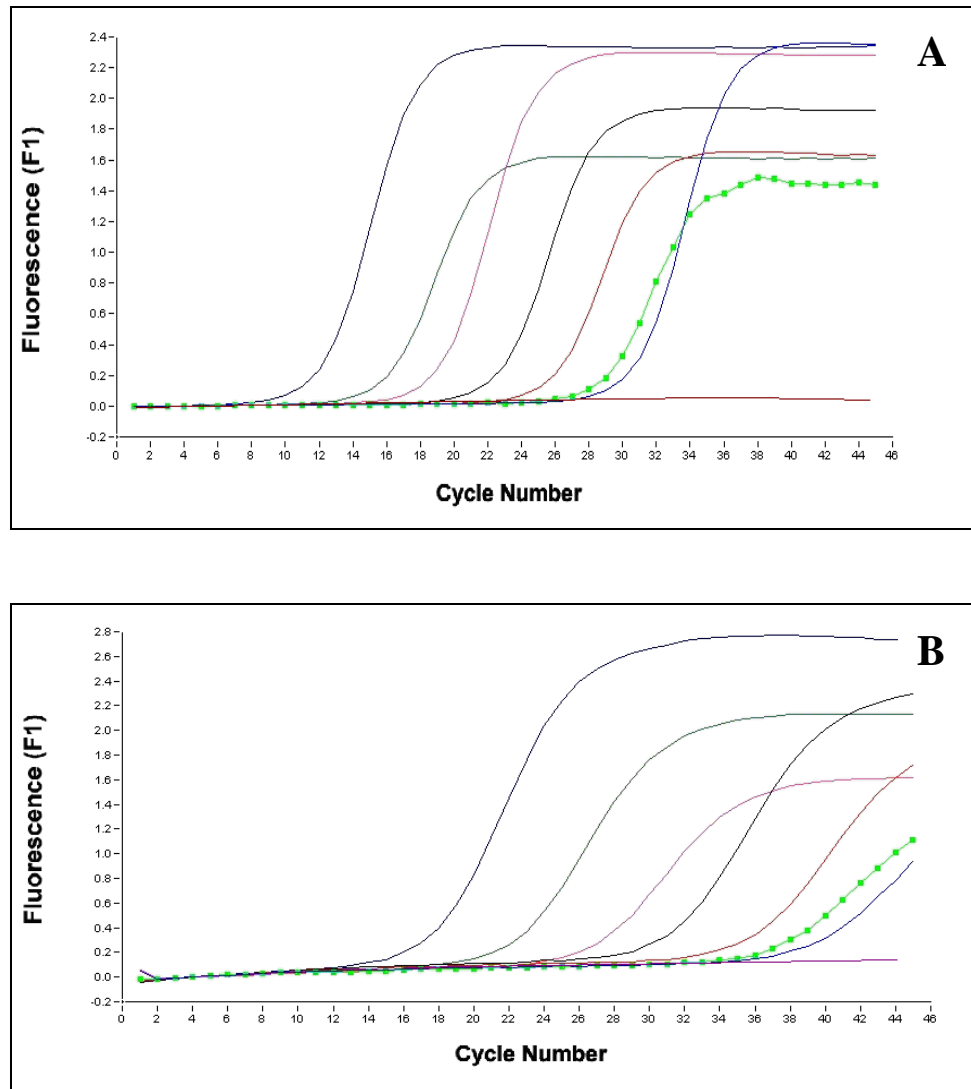


**Figure 15.** Real-time PCR amplification graph of standards of plasmid DNA extracted from transformed *E.coli* cells which were used for developing standard curves ( $2 \times 10^0$ – $2 \times 10^6$  gene copy number per 20  $\mu$ L of reaction) and no template control was included in qPCR reaction showing no unspecific amplification. **A**, amplified with CYA 107F and PICO 224R for general picos quantification; **B**, with CYA 107F and LSI 261R for LSI quantification.



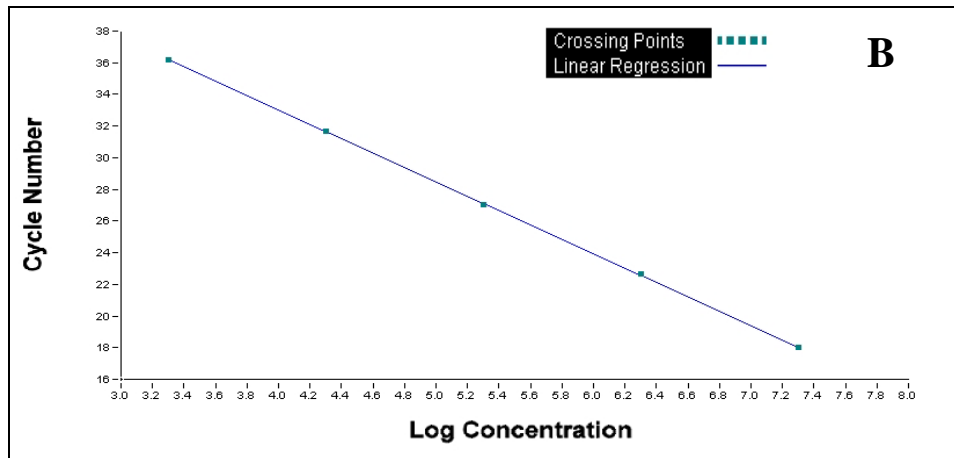
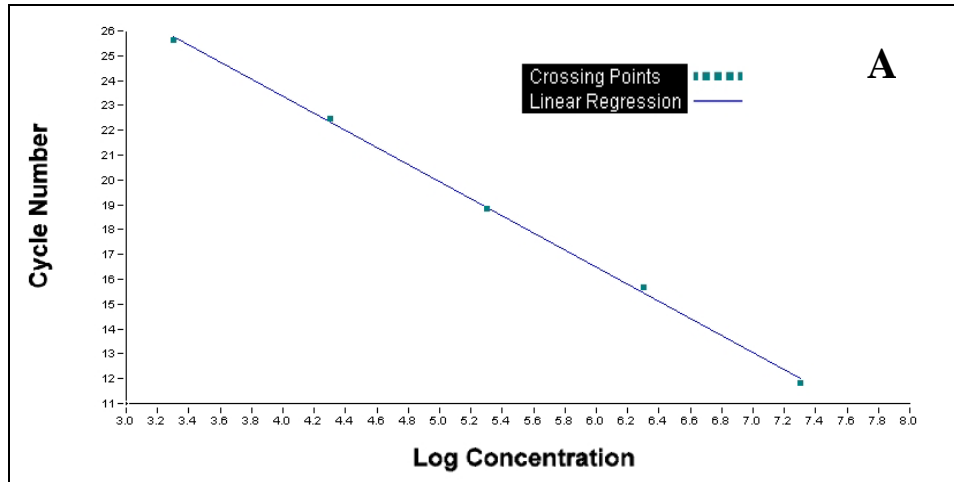


**Figure 16.** Standard curve for qPCR was determined as log concentration (DNA copy numbers / reaction) in correlation to cycle threshold (Ct). Serial dilutions of gene copy numbers of the cloned 16S rRNA ( $2 \times 10^2$ - $2 \times 10^6$  per 20  $\mu$ L of reaction) were included in the standard curve. Second derivative maximum was the analysis method used for quantification. A, amplified with CYA 107F and PICO 224R (general picos standard curve) with Slope: -3.435; B, with CYA 107F and LSI 261R (LSI standard curve) with Slope -4.540.

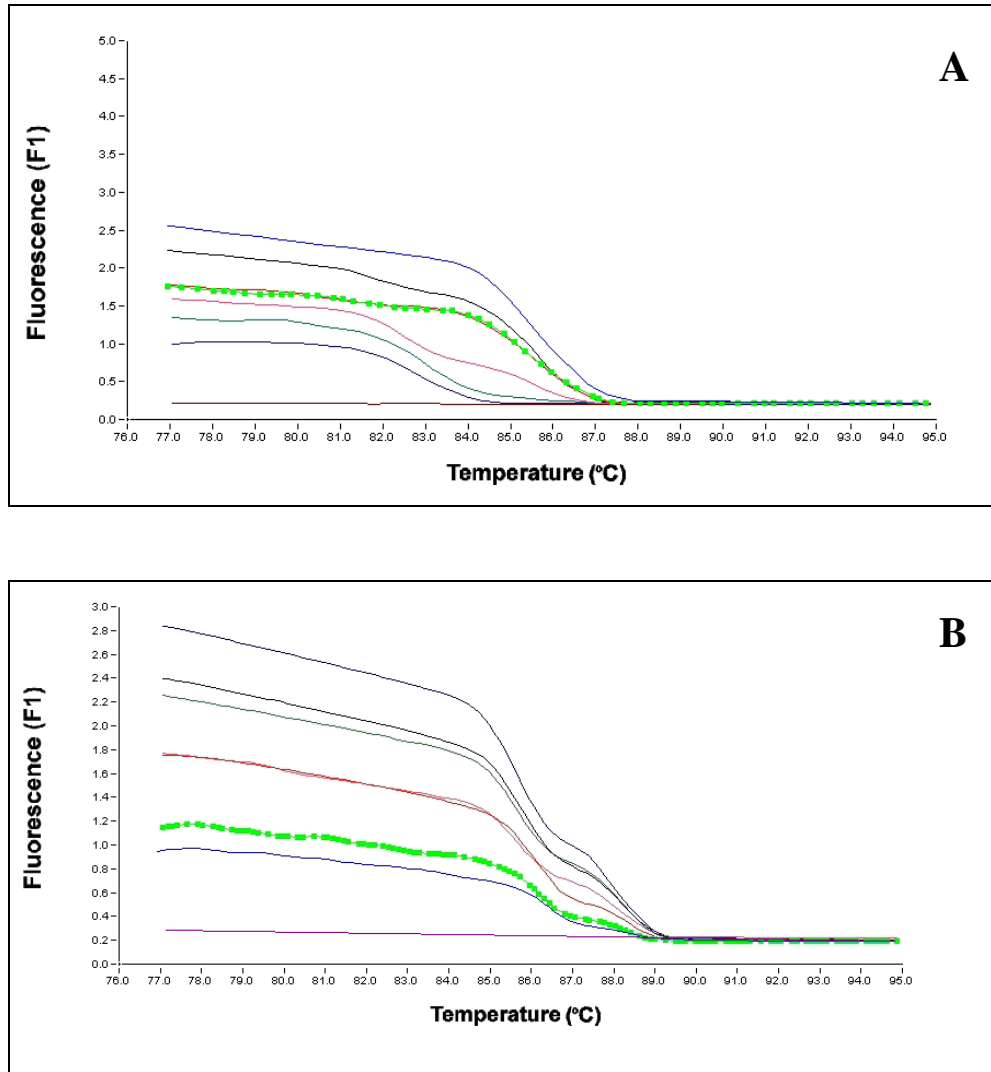


**Figure 17.** Melting curves of standards ( $2 \times 10^0$ – $2 \times 10^6$  copies/20  $\mu$ L); **A**, amplified with CYA 107F and PICO 224R of general picos standard curve; **B**, with CYA 107F and LSI 261R of LSI standard curve.

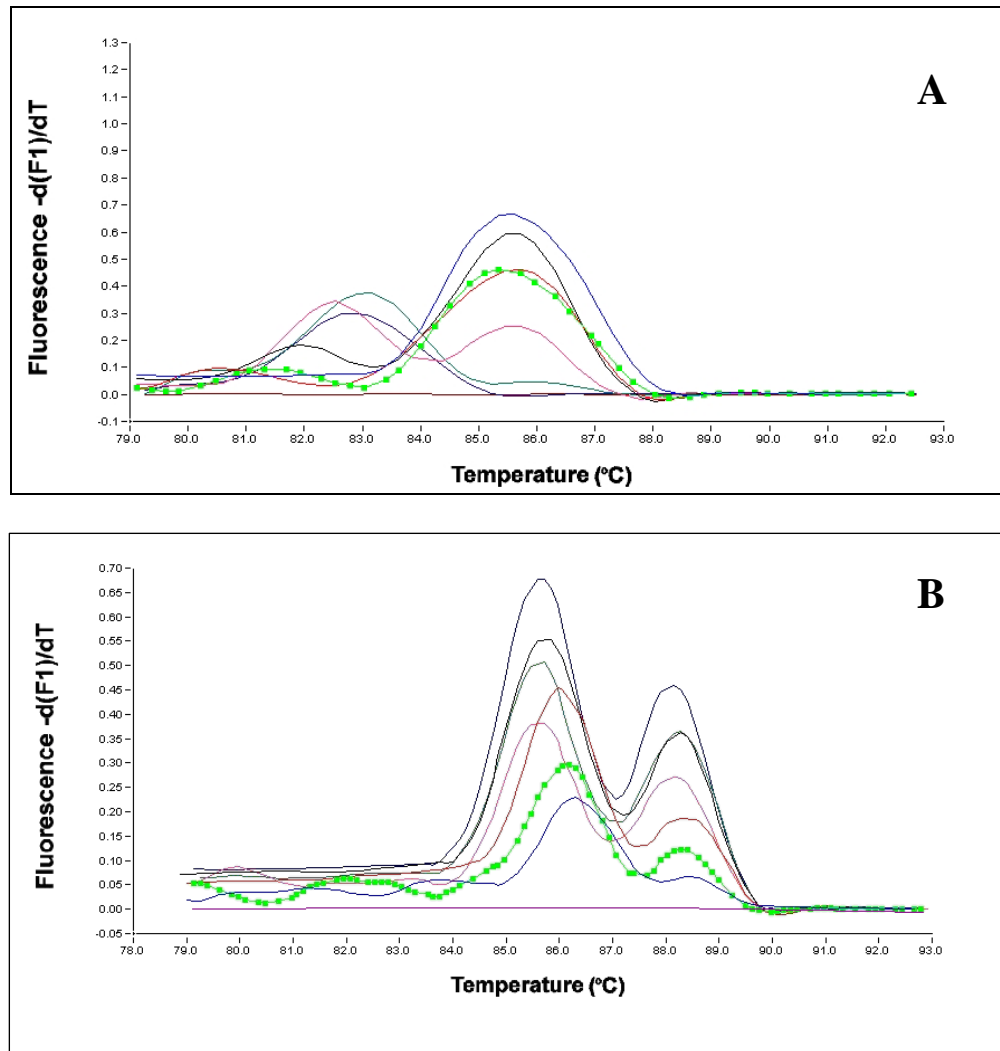


**Figure 18.** Melting curve analysis of standards amplified by real-time PCR showing no primer dimer fluorescence; **A**, amplified with CYA 107F and PICO 224R of general picos standard curve and the shift in  $T_m$  between standards of different concentrations was verified with another experiment (Figure 21); **B**, with CYA 107F and LSI 261R of LSI standard curve and the pattern of melting peak indicates the presence of position nucleotide variation in LSI strains present in the samples in comparison to the primer annealing sequence.

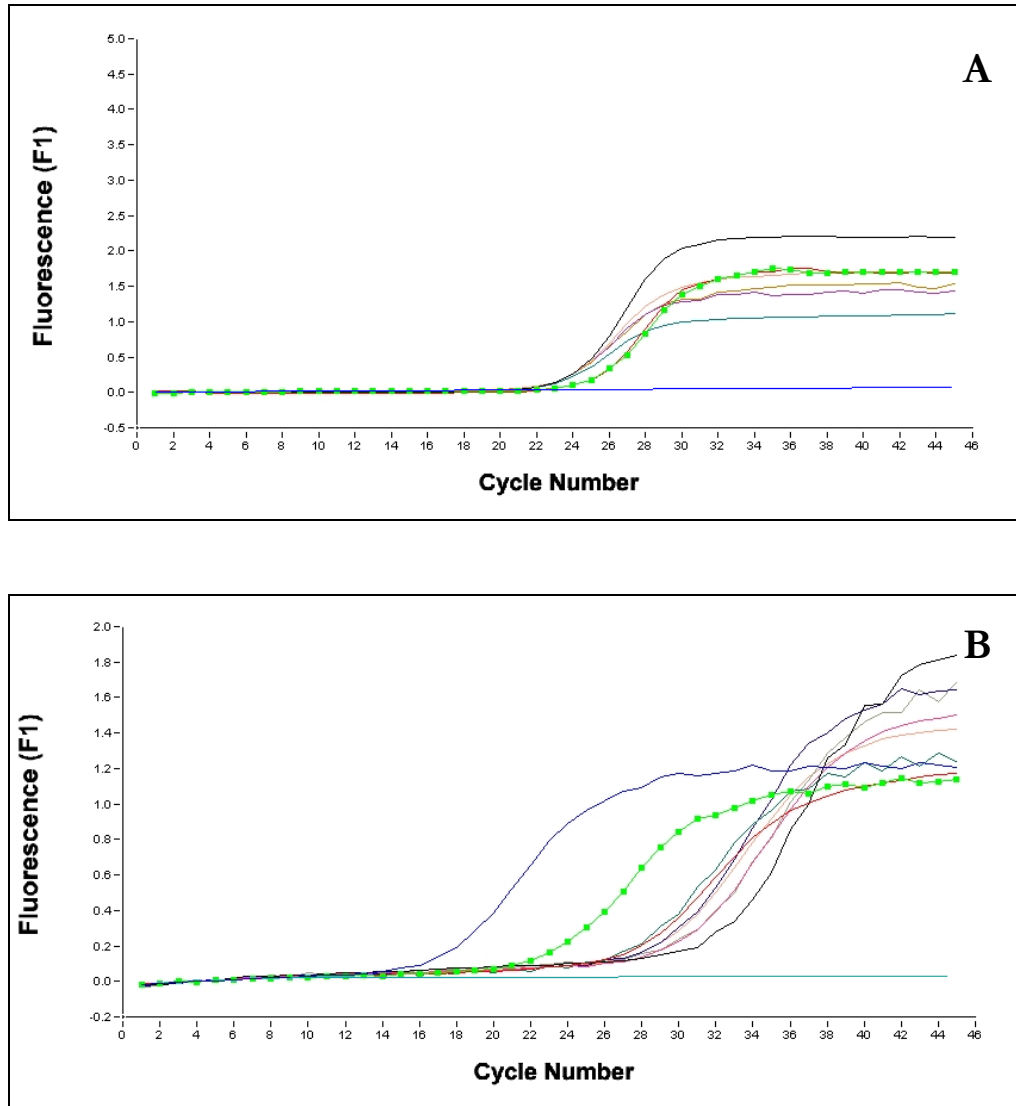


**Figure 19.** qPCR amplification graph of samples in which three standards were included in each run. A, show general picos quantification with standards ( $2 \times 10^1$ – $2 \times 10^3$  gene copies/20  $\mu$ L); B, LSI with standards ( $2 \times 10^4$ – $2 \times 10^6$  gene copies/20  $\mu$ L).

**Table 2.** Quantification of general picos 16S rRNA gene copy numbers and Ct values were obtained after acquiring external picos standard curve. PD samples are absent (consumed).

<b>Sample</b>	<b>Initial concentration (gene copies/20 <math>\mu</math>L of qPCR reaction)</b>	<b>Ct values</b>	<b>Calculated concentration (gene copies/20 <math>\mu</math>L of qPCR reaction)</b>
Standard	$2.0 \times 10^1$	24.87	$3.5 \times 10^1$
Standard	$2.0 \times 10^2$	24.72	$6.4 \times 10^1$
Standard	$2.0 \times 10^3$	23.64	$3.5 \times 10^3$
CD1	$2.3 \times 10^5$	22.71	$1.2 \times 10^5$
WM	$7.1 \times 10^5$	22.97	$4.5 \times 10^4$
SB	$6.9 \times 10^5$	22.90	$5.7 \times 10^4$
PD	---	---	---

**Table 3.** Quantification of LSI 16S rRNA gene copy numbers and Ct values were obtained after acquiring LSI external standard curve.

<b>Sample</b>	<b>Initial concentration (gene copies/20 <math>\mu</math>L of qPCR reaction)</b>	<b>Ct values</b>	<b>Calculated concentration (gene copies/20 <math>\mu</math>L of qPCR reaction)</b>
Standard	$2.0 \times 10^4$	27.97	$2.2 \times 10^4$
Standard	$2.0 \times 10^5$	23.52	$1.6 \times 10^5$
Standard	$2.0 \times 10^6$	17.68	$2.2 \times 10^6$
CD1	$2.3 \times 10^5$	31.23	$5.2 \times 10^3$
WM	$7.1 \times 10^5$	29.62	$1.1 \times 10^4$
SB	$6.9 \times 10^5$	30.04	$8.8 \times 10^3$
PD	$6.9 \times 10^4$	27.88	$2.3 \times 10^4$

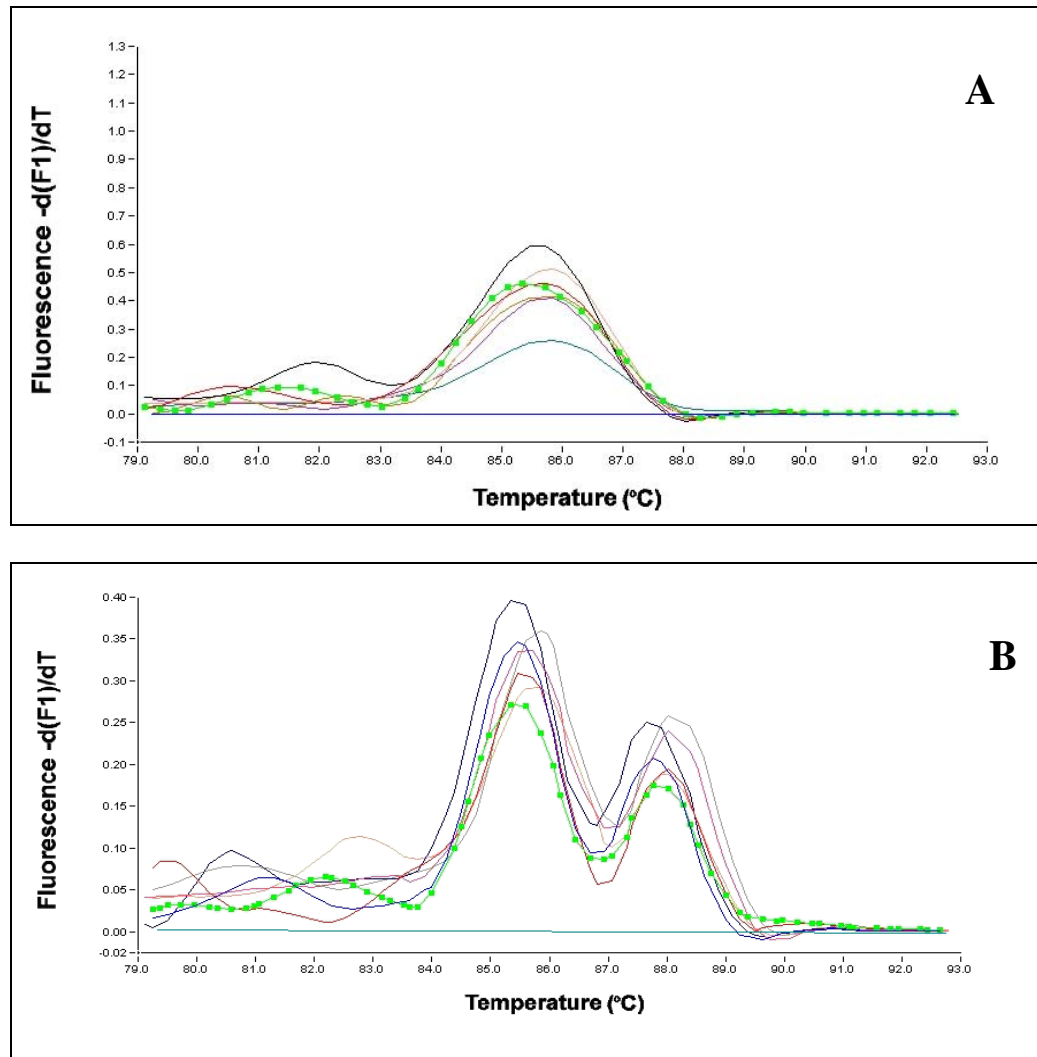


**Figure 20.** Melting curve analysis of samples and three standards were included in qPCR reaction showing reproducible pattern of peaks. **A**, represents melting peaks of picos samples and standards ( $2 \times 10^1$ – $2 \times 10^3$  gene copies/ $20 \mu L$ ); **B**, LSI and standards ( $2 \times 10^4$ – $2 \times 10^6$  gene copies/ $20 \mu L$ ).

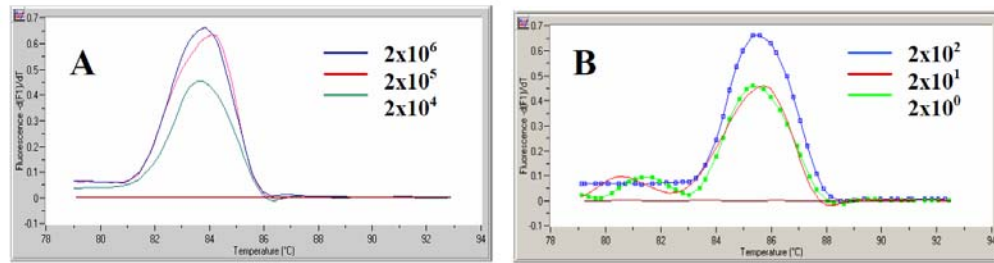


**Figure 21.** Melting curve analysis of standards used to build the standard curve of general picos with CYA 107F and PICO 224R primers showing. No template control was included in the reaction showing no unspecific amplification. **A**, includes standards  $2 \times 10^4$ – $2 \times 10^6$  gene copies/20  $\mu$ L with  $T_m$  (81–86  $^{\circ}$ C); **B**,  $2 \times 10^0$ – $2 \times 10^2$  gene copies/20  $\mu$ L with  $T_m$  (83–88  $^{\circ}$ C). Melting peaks are obtained from the same real-time PCR run. DNA concentration shows a slight influence on melting temperature.

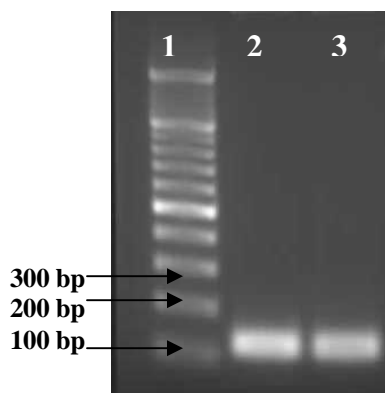


**Figure 22.** Amplification with CYA 107F and PICO 224R viewed by 1% agarose gel electrophoresis showing exact amplicon size of both amplified DNA of standards and samples (118 bp). Lane 1, genomic DNA from sample CD1 (50 ng); Lane 2, plasmid DNA (25 ng) from transformed *E.coli* cells used for building the standard curve of general picocyanobacteria.

### 3.4 General picos and LSI gene copy numbers of the 16S rRNA per mL of filtered water from Lake Superior

Final qPCR results of LSI and picos cells at different hydrographic locations of Lake Superior were reported as gene copy number per mL of filtered water (Table 4). LSI was more concentrated at PD and WM whereas picos were more concentrated at CD1 and WM (Figure 23). The picos community concentration was not assessed at location PD since the sample was completely consumed.

**Table 4.** Gene copy numbers (16S rRNA) of general picos and LSI per mL of filtered water from several locations of Lake Superior.

Location	Date of collection	Depth (m)	Filtered Volume (mL)	Gene copy numbers/20 $\mu$ L of qPCR (picos)	Gene copy number/mL of filtered water (picos)	Gene copy number/20 $\mu$ L of qPCR (LSI)	Gene copy number/mL of filtered water (LSI)
<b>CD1</b>	14/09/2004	5	450	$1.2 \times 10^5$	$2.7 \times 10^3$	$5.2 \times 10^3$	$1.2 \times 10^2$
<b>WM</b>	15/09/2004	30	450	$4.5 \times 10^4$	$1.0 \times 10^3$	$1.1 \times 10^4$	$2.4 \times 10^2$
<b>SB</b>	14/09/2004	5	1500	$5.7 \times 10^4$	$3.8 \times 10^2$	$8.8 \times 10^3$	$5.9 \times 10^1$
<b>PD</b>	16/09/2004	7	450	---	---	$2.3 \times 10^4$	$5.1 \times 10^2$



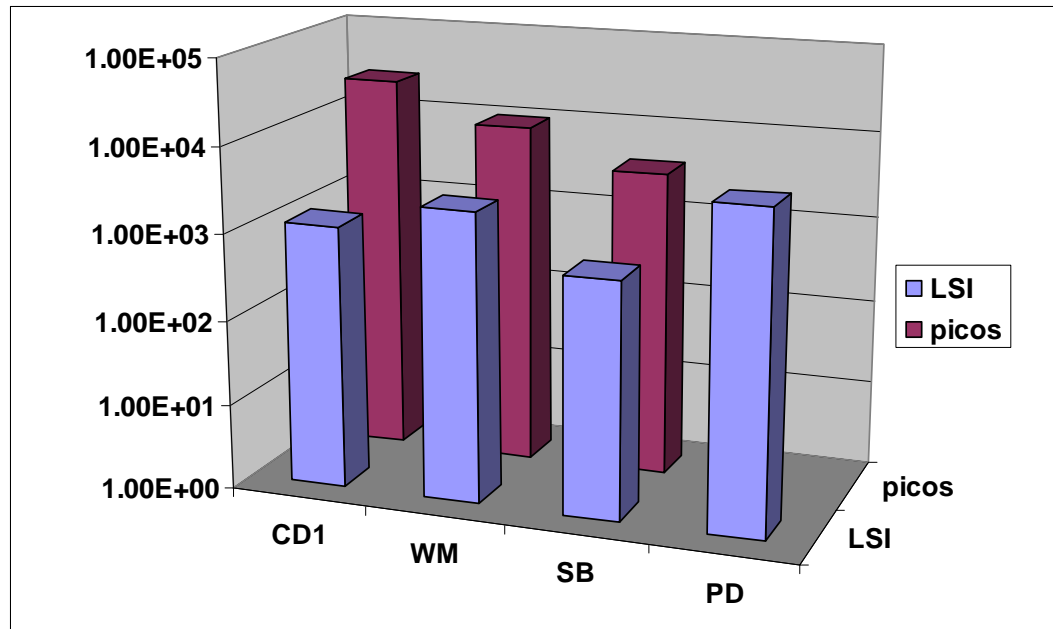


**Figure 23.** Distribution and correlation of picos and LSI in relation to the same location of Lake Superior as a function of gene copy number/mL of filtered water collected from Lake Superior.

## Chapter IV

### DISCUSSION

#### 4.1 qPCR standard curves and melting curve analysis

We have mentioned earlier that strains cluster within LSI were not isolated into cyanobacteria cultures. This made us clone this specific sequence to a vector followed by transformation into *E.coli* competent cells. The vectors were used later on to generate the qPCR standard curve. Since we also aim to generally estimate the proportion of LSI of the general picos, both qPCR used to quantify the picos and LSI included exactly the same DNA and reagent concentrations, qPCR cycling conditions, and forward primer (CYA 107F).

The patterns of melting peaks for all samples and standards of LSI showed two-shoulder peak (Figures 18; B & 20; B) which is an indication of single nucleotide variation in the specific sequence targeted (Elenitoba-Johnson *et al.*, 2001; Lipsky *et al.*, 2001). Since SYBR Green I is not highly sequence specific to confirm the sequence variation (Zipper *et al.*, 2004), we examined all 290 sequences identified by Ivanikova *et al.* (2007) and 1 to 4 nucleotide differences along the 23 bp 16S rRNA sequence were detected (Table 5). The pattern of melting peaks can be confirmed with specific TaqMan assays (Sánchez-Baracaldo *et al.*, 2008).

**Table 5.** One nucleotide difference in LSI 261R annealing sequence detected from Lake Superior isolates by Ivanikova *et al.* (2007); labeled in black color. Two to four nucleotide differences are not shown. Sequences were provided by the corresponding author Dr. George Bullerjahn.

Specific LSI original sequence	<b>5'-GGTAAGGTAATGGCTTACCAAG-3'</b>
LS399_WM_Sep_5m_5-B3	<b>5'-GGTAAGGTAATGGTTTACCAAG-3'</b>
LS149_SB_May_5m_6-C7	<b>5'-GGTAAGGTAACGGCTTACCAAG-3'</b>

When building the standard curve, specific for quantifying picos, we noticed a shift in  $T_m$  between low and high DNA concentrations (Figure 18; A). This was not recognized in cyanobacteria samples which contain the same amount of starting template DNA. Hence, we assumed that template concentration influence the  $T_m$ . This was verified by a separate experiment including both low and high DNA concentrations of standards and a slight shift in  $T_m$  was noticed (Figure 21). A recent article by Schütz and Ahsen (2009) showed a shift in  $T_m$  by varying template DNA concentration. The free energy, enthalpy, and entropy from dsDNA melting curves have an effect on primer binding. This infers primer specificity which reasons the fact that the  $T_m$  shift was not shown with the other reverse primer used in qPCR of LSI. Moreover, the PCR product has also an influence on the melting peaks. Therefore, the fact that the  $T_m$  shift was not observed with LSI reverse primer was possibly due to the higher PCR product obtained from quantifying picos compared to LSI PCR product (Table 4).

Another explanation might be due to sequence variation which causes a shift in  $T_m$  (Germer and Higuchi, 1999). Sequence variation might be present in very low amount in the standards. This explains the fact that it has been

observed only in standards of high concentrations of DNA copy numbers which did not match with the sample melting peaks. This phenomenon originated from early cloning where the amplified sequence by CYA 107F and LSI 258R has amplified the sequence recognized by PICO 224R (general picos sequence) of several picos isolates. These picos general sequences contained slight position nucleotide variation (Table 6). Since each 16S rRNA clone develop into single colony, we might have inadvertently included two sequences with slight variation in DNA sequence as a result of attached colonies of the 16S rRNA clones. We have examined all sequences provided by Dr. George Bullerjahn and found that 40 out of 290 isolates of the general picos did not match perfectly with the PICO 224 annealing sequence (Table 6). Since these sequences are present in very little amount, they did not occur in the qPCR of samples.

**Table 6.** Sequence variation detected in PICO 224R annealing sequence of Ivanikova *et al.* (2007) picos which were provided by the corresponding author Dr. George Bullerjahn. Only 5 of 40 sequences that did not match with the PICO 224 annealing sequence are displayed. Nucleotide difference is labeled in black.

Specific picos general sequence	5'-CCTGAGGATGAGCTCGCGT-3'
LS377_CD1_Sep_5m_4-H5	5'-CTT <b>G</b> AGGATGAGCTCGCGT-3'
LS160_SB_May_5m_6-D6	5'-CCTGAGGATGG <b>G</b> CTCGCGT-3'
LS34_PD_Sep_5m_7-C10	5'-CCTGAGGATGG <b>CC</b> CGCGT-3'
LS324_WM_Sep_30m_4-C12	5'-CC <b>G</b> AGGGATGAGCTCGCGT-3'

## 4.2 Distribution of picos and LSI in Lake Superior

This study is the first that genetically quantify the general picos and the novel LSI of Lake Superior. Gene copy numbers/mL ( $2.7 \times 10^3$ ) of picos obtained by this study from location CD1 at 5 m (September, 2004) are in the range of flow cytometry results shown by Ivanikova *et al.* (2007) of PC-rich APP and PE-rich APP collected from CD1 (August, 2006) which are  $<10^3$  and  $1.30 \times 10^4$  cells/mL respectively. After comparing our results of samples collected in September 2004 to flow cytometry results in August 2006 (Ivanikova *et al.*, 2007), we noticed an increase in the APP community at the epilimnion (5 m) of CD1 in August (2006).

In agreement with Ivanikova *et al.* (2007) our qPCR results infer that LSI isolates are primarily present at offshore Lake Superior stations including CD1, SB, and WM (Figure 26). Ivanikova *et al.* (2007) indicates that at nearshore station PD only 4% of sequences clustered within LSI which was less abundant than other hydrographic stations. Conversely, we found that PD was also highly populated with LSI compared to concentrations obtained from other hydrographic stations (Figure 26). Since nearshore PD showed the highest levels of LSI, we suggest that LSI sequences isolated by Ivanikova *et al.* (2007) were diluted in a large population of picos consisting of high genetic diversity. The shallow nearshore station PD was found to be more genetically diverse than the pelagic community. Members of the *C. gracile* cluster, group B (subalpine cluster I), the Lake Biwa cluster sensu Ernst *et al.* (2003), group H, and two novel minor PD-specific clusters (PDI and PDII) were all detected in nearshore PD (Ivanikova *et al.*, 2007).

Samples from hydrographic stations of CD1, PD, and SB were collected from the epilimnion at 5 m depth. However, WM which was collected at deep chlorophyll maximum (DCM) at 30 m depth showed also the same trend of LSI being a major group in picos. Most sequences isolated at WM by Ivanikova *et al.* (2007) clustered within LSI.

In general, LSI was more concentrated at stations WM and PD (Table 4). However, CD1 station showed higher levels of picos than WM and SB (PD was not assessed). LSI form major fraction of general picos community at several locations of Lake Superior including CD1 (4.4%), WM (24%), and SB (15.5%). These percentages should not be underestimated since Ivanikova *et al.* (2007) showed that 16S rRNA sequences of picocyanobacteria at the western arm of the lake were highly diverse.

### **4.3 Conclusions**

Picocyanobacteria are a genetically diverse community. The optimized and specific qPCR protocol generated by this study allows the assessment of spatial and temporal abundance of general picos and LSI in filtered water samples. Our study provides valuable information on the dynamics of general picos and LSI in Lake Superior as an example of oligotrophic and freshwater lake.

### **4.4 Future outlook**

We recommend applying this protocol to a wider scale of samples from Lake Superior collected at different seasonal dates. The picos results can be confirmed by using an isolate of *Synechococcus* sp. that contains the general

16S rRNA sequence of this group to build a qPCR standard curve. Future studies can focus on culturing techniques to isolate picocyanobacteria that cluster within LSI. Ivanikova *et al.* (2007) indicated that most of the libraries isolated belong to LSI and LSII; therefore, it is worthy to quantify LSII by generating a qPCR that is similar to what we have accomplished in this study. A better comprehension of the APP dynamics and diversity will only be accomplished by quantifying all sequences isolated from Lake Superior by which our study is only a modest step towards this mission.

## Chapter VI

### BIBLIOGRAPHY

- Applied Biosystems. *Real-time PCR vs. traditional PCR*. Retrieved September 19<sup>th</sup>, 2009, from: [http://www.appliedbiosystems.com/support/tutorials/pdf/rtpcr\\_vs\\_tradpcr.pdf](http://www.appliedbiosystems.com/support/tutorials/pdf/rtpcr_vs_tradpcr.pdf).
- Bailey-Watts, A.E., Bindloss, M.E., & Belcher, J.H. (1968). Freshwater primary production by a blue-green algae of bacterial size. *Nature*, 220, 1344-1345.
- Becker, S., Fahrbach, M., Böger, P., & Ernst, A. (2002). Quantitative tracing, by taq nuclease assays, of a *Synechococcus* ecotype in a highly diversified natural population. *Applied and Environmental Microbiology*, 68(9), 4486-4494.
- Bell, T., & Kalff, L. (2001). The contribution of picophytoplankton in marine and freshwater systems of different trophic status and depth. *Limnology and Oceanography*, 46, 1243-1248.
- Bhattacharya, D., & Medlin, L. (1998). Algal phylogeny and the origin of land plants. *Plant Physiology*, 116, 9-15.
- Brasier, M., Green, O., Lindsay, J., & Steele, A. (2004). Earth's oldest (3.5 Ga) fossils and the 'Early Eden hypothesis': Questioning the evidence. *Origins of Life and Evolution of the Biosphere*, 34, 257-269.



- Callieri, C. (2007). Picophytoplankton in freshwater ecosystems: the importance of small-sized phototrophs. *Freshwater Reviews*, *1*, 1-28.
- Callieri, C., Corno, G., Caravati, E., Galafassi, S., Bottinelli, M., & Bertoni, R. (2007). Photosynthetic characteristics and diversity of freshwater *Synechococcus* at two depths during different mixing conditions in a deep oligotrophic lake. *Journal of Limnology*, *66*(2), 81-89.
- Callieri, C., Morabito, G., Huot, Y., Neal, P., & Lichman, E. (2001). Photosynthetic response of pico- and nanoplanktonic algae to UVB, UVA and PAR in a high mountain lake. *Aquatic Sciences*, *63*(3), 286-293.
- Callieri, C., & Stockner, J.G. (2002). Freshwater autotrophic picoplankton: A review. *Journal of Limnology*, *61*(1), 1-14.
- Caron, D.A. (1983). Technique for enumeration of heterotrophic and phototrophic nanoplankton, using epifluorescence microscopy, and comparison with other procedures. *Applied and Environmental Microbiology*, *46*(2), 491-498.
- Caron, D.A., Pick, F.R., & Lean, D.R.S. (1985). Chroococcoid cyanobacteria in Lake Ontario: seasonal and vertical distribution during 1982. *Journal of Phycology*, *21*, 171-175.
- Chisholm, S.W., Olson, R.J., Zettler, E.R., Goericke, R., Waterbury, J.B., & Welschmeyer, N.A. (1988). A novel free-living prochlorophyte abundant in the oceanic euphotic zone. *Nature*, *334*, 340-343.

- Church, M.J., Björkman, K.M., Karl, D.M., Saito, M.A., & Zehr, J.P. (2008). Regional distributions of nitrogen-fixing bacteria in the Pacific Ocean. *Limnology Oceanography*, 53(1), 63-77.
- Crosbie, N.D., Pöckl, M., & Weisse, T. (2003a). Dispersal and phylogenetic diversity of nonmarine picocyanobacteria, inferred from 16S rRNA gene and *cpcBA*-intergenic spacer sequence analyses. *Applied and Environmental Microbiology*, 69(9), 4055-4065.
- Crosbie, N.D., Teubner, K., & Weisse, T. (2003b). Flow-cytometric mapping provides novel insights into the seasonal and vertical distributions of freshwater autotrophic picoplankton. *Aquatic Microbial Ecology*, 33(1), 53-66.
- Czeczuga, B. (1985). Light-harvesting phycobiliprotein pigments of the red algae *Leptosomia simplex* from the Antarctic. *Polar Biology*, 4, 179-189.
- Diaz, M., Pedrozo, F., Reynolds, C., & Temporetti, P. (2007). Chemical composition and the nitrogen-regulated trophic state of Patagonian lakes. *Limnologica*, 37, 17-27.
- Elenitoba-Johnson, K.S.J., & Bohling, S.D. (2001). Solution-Based Scanning for Single-base alterations using a double-stranded DNA binding dye and fluorescence-melting profiles. *American Journal of Pathology*, 159(3), 849-853.

- Ernst, A., Becker, S., Wollenzien, U.A., & Postius, C. (2003). Ecosystem-dependent adaptive radiations of picocyanobacteria inferred from 16S rRNA and ITS-1 sequence analysis. *Microbiology*, *149*, 217-228.
- Erokhina, L.G., Spirina, E.V., Shatilovich, A.V., & Gilichinskii, D.A. (2004). Chromatic adaptation of viable ancient cyanobacteria from arctic permafrost. *Microbiology*, *69*(6), 730-731.
- Everroad, R.C., & Wood, A.M. (2006). Comparative molecular evolution of newly discovered picocyanobacterial strains reveals a phylogenetically informative variable region of  $\beta$ -phycoerythrin. *Journal of Phycology*, *42*, 1300-1311.
- Fahnenstiel, G.L., Sicko-Goad, L., Scavia, D., & Stoermer, S.E. (1986). Importance of phytoplankton in Lake Superior. *Canadian Journal of Fisheries and Aquatic Sciences*, *43*, 235-240.
- Flores, E., Frías, F.E., Rubio, L.M., & Herrero, A. (2005). Photosynthetic nitrate assimilation in cyanobacteria. *Photosynthesis Research*, *83*, 117-113.
- Furukawa, K., Noda, N., Tsuneda, S., Saito, T., Itayama, T., & Inamori, Y. (2006). Highly sensitive real-time PCR assay for quantification of toxic cyanobacteria based on Microcystin Synthetase A Gene. *Journal of Bioscience and Bioengineering*, *102*(2), 90-96.
- Garcia-Pichel, F., Nübel, U., & Muyzer, G. (1998). The phylogeny of unicellular, extremely halotolerant cyanobacteria. *Archives of Microbiology*, *169*(6), 469-482.

- Germer, S., & Higuchi, R. (1999). Single-tube genotyping without oligonucleotide probes. *Genome Research*, *9*, 72-78.
- Giovannoni, S.J., Turner, S., Olsen, G.J., Barns, S., Lane, D.J., & Pace, N.R. (1988). Evolutionary relationships among cyanobacteria and green chloroplasts. *Journal of Bacteriology*, *170*(2), 3584-3592.
- Haverkamp, T., Acinas, S.G., Doeleman, M., Stomp, M., Huisman, J., & Stal, L.J. (2008). Diversity and phylogeny of Baltic Sea picocyanobacteria inferred from their ITS and phycobiliprotein operons. *Environmental Microbiology*, *10*, 174-188.
- Ivanikova, N.V. (2006). *Lake Superior phototrophic picoplankton: Nitrate assimilation measured with a cyanobacteria nitrate-responsive bioreporter and genetic diversity of the natural community*. Unpublished doctoral dissertation, Bowling Green State University, Ohio, U.S.A
- Ivanikova, N.V., Popels, L.C., McKay, M.L., & Bullerjahn, G.S. (2007). Lake superior supports novel clusters of cyanobacterial picoplankton. *Applied and Environmental Microbiology*, *73*(12), 4055-4065.
- Jezberová, J., & Komárková, J. (2007). Morphological transformation in a freshwater *Cyanobium* sp. induced by grazers. *Environmental Microbiology*, *9*(7), 1858-1862.

- Koskenniemi, K., Lyra, C., Rajaniemi-Wacklin, P., Jokela, J., & Sivonen, K. (2007). Quantitative real-time PCR detection of toxic *Nodularia* cyanobacteria in the Baltic Sea. *Applied and Environmental Microbiology*, *73*(7), 2173-2179.
- Li, W.K.W., Subba Rao, D.V., Harrison, W.G., Smith, J.C., Cullen, J.J., Irwin, B., et al. (1983). Autotrophic picoplankton in the tropical ocean. *Science*, *219*(4582), 292-295.
- Lipsky, R.H., Mazzanti, C.M., Rudolph, J.G., Xu, K., Vyas, G., Bozak, D., et al. (2001). DNA melting analysis for detection of single nucleotide polymorphisms. *Clinical Chemistry*, *47*(4), 635-644.
- Malinen, E., Kassinen, A., Rinttilä, T., & Palva, A. (2003). Comparison of real-time PCR with SYBR Green I or 59-nuclease assays and dot-blot hybridization with rDNA-targeted oligonucleotide probes in quantification of selected faecal bacteria. *Microbiology*, *149*, 269-277.
- Manen, J., & Falquet, J. (2002). The *cpcB-cpcA* locus as a tool for the genetic characterization of the genus *Arthrospira* (Cyanobacteria): Evidence for horizontal transfer. *International Journal of Systematic and Evolutionary Microbiology*, *52*, 861-867.
- Mariné, M.H, Clavero, E., & Roldán, M. (2004). Microscopy methods applied to research on cyanobacteria. *Limnetica*, *23*(1-2): 179-186.

- Marsac, N.T.D. (1977). Occurrence and nature of chromatic adaptation in cyanobacteria. *Journal of Bacteriology*, 130(1): 82-91.
- Matheson, D.H., & Munawar, M. (1978). Lake Superior basin and its development. *Journal of Great Lakes Research*, 4, 249-263.
- Moser, M., Callieri, C., & Weisse, T. (2009). Photosynthetic and growth response of freshwater picocyanobacteria are strain-specific and sensitive to photoacclimation. *Journal of Plankton Research*, 31(4), 349-357.
- Nubel, U., Garcia-Pichel, F., & Muyzer, G. (1997). PCR primers to amplify 16S rRNA genes from cyanobacteria. *Applied and Environmental Microbiology*, 63(8), 3327-3332.
- Passoni, S., & Callieri, C. (2001). Picocyanobacteria single forms, aggregates and microcolonies: Survival strategy or species succession? *Verhandlungen der Internationale Vereinigung für theoretische und angewandte Limnologie*, 27, 1879-1883.
- Robertson, B.R., Tezuka, N.R., & Watanabe, M.M. (2001). Phylogenetic analyses of *Synechococcus* strains (cyanobacteria) using sequences of 16S rDNA and part of the phycocyanin operon reveal multiple evolutionary lines and reflect phycobilin content. *International Journal of Systematic and Evolutionary Microbiology*, 51, 861-871.

- Roche. (2000, November). *Light Cycler absolute quantification with external standards*. Retrieved September 25<sup>th</sup>, 2009, from: <http://www.gene-quantification.org/roche-ex-standards.pdf>.
- Rudi, K., Skulberg, O.M., & Jakobsen, K.S. (1998). Evolution of cyanobacteria by exchange of genetic material among phylogenically related strains. *Applied and Environmental Microbiology*, *180*(13), 3453-3461.
- Sánchez-Baracaldo, P., Handley, B.A., & Hayes, P.K. (2008). Picocyanobacterial community structure of freshwater lakes and the Baltic Sea revealed by phylogenetic analyses and clade-specific quantitative PCR. *Microbiology*, *154*, 3347-3357.
- Sato, N., Ishikawa, M., Fujiwara, M., & Sonoike, K. (2005). Mass identification of chloroplast proteins of endosymbiont origin by phylogenetic profiling based on organism-optimized homologous protein groups. *Genome Informatics*, *16*(2), 56-68.
- Scanlan, D.J., & West, N.J. (2002). Molecular ecology of the marine cyanobacterial genera *Prochlorococcus* and *Synechococcus*. *FEMS Microbiology Ecology*, *40*, 1-12.
- Schindler, D. W. (2006). Recent advances in the understanding and management of eutrophication. *Limnology and Oceanography*, *51*(2), 356-363.

- Shi, T., & Falkowski, P.G. (2007). Genome evolution in cyanobacteria: The stable core and the variable shell. *Proceedings of the National Academy of Sciences*, *105*(7), 2510-2515.
- Stal, L.J., & Krumbein, W.E. (1987). Temporal separation of nitrogen fixation and photosynthesis in the filamentous, non-heterocystous cyanobacteria *Oscillatoria* sp. *Archives of Microbiology*, *149*, 76-80.
- Steinberg, C.E.W., & Hartmann, H.M. (1988). Planktonic bloom-forming Cyanobacteria and the eutrophication of lakes and rivers. *Freshwater Biology*, *20*, 279-287.
- Stockner, J.G., Callieri, C., & Cronberg, G. (2000). Picoplankton and other non-bloom forming cyanobacteria in lakes. In B. Whitton & M. Potts (Eds.), *The ecology of cyanobacteria: Diversity in time in space* (pp. 195-231). The Netherlands: Kluwer Academic Publishers.
- Ting, C.S., Rocap, G., King, J., & Chisholm, S.W. (2002). Cyanobacterial photosynthesis in the oceans: The origins and significance of divergent light-harvesting strategies. *Trends in Microbiology*, *10*(3), 134-142.
- Tomitani, A., Knoll, A.H., Cavanaugh, C.M., & Ohno, T. (2006). The evolutionary diversification of cyanobacteria: Molecular-phylogenetic and paleontological perspectives. *Proceedings of the National Academy of Sciences*, *103*(14), 5442-5447.



- Urbach, E., Scanlan, D.J., Distel, D.L., Waterbury, J.B., & Chisholm, S.W. (1998). Rapid diversification of marine picophytoplankton with dissimilar light-harvesting structures inferred from sequences of *Prochlorococcus* and *Synechococcus* (Cyanobacteria). *Journal of Molecular Evolution*, 46(2), 188-201.
- Walsby, A.E., Hayes, P.K., & Boje, R. (1995). The gas vesicles, buoyancy and vertical distribution of cyanobacteria in the Baltic Sea. *European Journal of Phycology*, 30, 87-94.
- Waterbury, J.B., & Rippka, R. (1989). Subsection I. Order Chroococcales Wettstein 1924, Emend. Rippka *et al.* 1979. In J.T. Staley, M.P. Bryant, N. Pfennig, & J.G. Holt (Eds.), *Bergey's manual of systematic bacteriology* (Vol. 3. pp. 1748-1725). Baltimore: Williams and Wilkins.
- Weiler, R.R. (1978). Chemistry of Lake Superior. *Journal of Great Lakes Research*, 4, 370-385.
- Zipper, H., Brunner, H., Bernhagen, J., & Vitzthum, F. (2004). Investigations on DNA intercalation and surface binding by SYBR Green I, its structure determination and methodological implications. *Nucleic Acids Research*, 32(12). Retrieved September 20<sup>th</sup>, 2009, from: <http://nar.oxfordjournals.org/cgi/content/full/32/12/e103>.

